Trans-Omics analysis of post injury thrombo-inflammation identifies endotypes and trajectories in trauma patients.

Authors: Mitchell J. Cohen[1]†, Christopher B. Erickson[1,2]†, Ian S. Lacroix[2], Margot Debot[1], Monika Dzieciatkowska[2], Terry R. Schaid[1], Morgan W. Hallas[1], Otto N. Thielen[1], Alexis L. Cralley[1], Anirban Banerjee[1], Ernest E Moore[1,3], Christopher C. Silliman[1,4,5,6], Angelo D'Alessandro[2*‡], Kirk C. Hansen[2*‡]

Affiliations:

[1]Department of Surgery, University of Colorado Anschutz Medical Campus; Aurora, CO.

[2]Department of Biochemistry and Molecular Genetics, University of Colorado Anschutz Medical Campus; Aurora, CO.

[3]Denver Health Medical Center; Denver, CO.

[4]Department of Pediatrics, University of Colorado Anschutz Medical Campus; Aurora, CO.

[5]Vitalant Research Institute; Denver, CO.

[6]Center for Cancer and Blood Disorders, Children's Hospital of Colorado; Aurora, CO.

†Co-first authors. These authors contributed equally to this manuscript.

‡Co-senior authors. These authors managed all data accumulation and analyses.

*Co-Corresponding authors: kirk.hansen@cuanschutz.edu; angelo.dalessandro@cuanschutz.edu

One-sentence summary: Transomic analyses of longitudinal plasma samples from severely injured patients identifies endotypes and trajectories that predict clinical outcomes.

Running title: Omics-informed trauma endotypes

ABSTRACT

Understanding and managing the complexity of trauma-induced thrombo-inflammation necessitates an innovative, data-driven approach. This study leveraged a trans-omics analysis of longitudinal samples from trauma patients to illuminate molecular endotypes and trajectories that underpin patient outcomes, transcending traditional demographic and physiological characterizations. We hypothesize that trans-omics profiling reveals underlying clinical differences in severely injured patients that may present with similar clinical characteristics but ultimately have very different responses to treatment and clinical outcomes. Here we used proteomics and metabolomics to profile 759 of longitudinal plasma samples from 118 patients at 11 time points and 97 control subjects. Results were used to define distinct patient states through data reduction techniques. The patient groups were stratified based on their shock severity and injury severity score, revealing a spectrum of responses to trauma and treatment that are fundamentally tied to their unique underlying biology. Ensemble models were then employed, demonstrating the predictive power of these molecular signatures with area under the receiver operating curves of 80 to 94% for key outcomes such as INR, ICU-free days, ventilator-free days, acute lung injury, massive transfusion, and death. The molecularly defined endotypes and trajectories provide an unprecedented lens to understand and potentially guide trauma patient management, opening a path towards precision medicine. This strategy presents a transformative framework that aligns with our understanding that trauma patients, despite similar clinical presentations, might harbor vastly different biological responses and outcomes.

INTRODUCTION

Trauma and hemorrhage remain a leading cause of death worldwide (*1, 2*). Underlying this mortality and the prime cause of morbidity in survivors is a poorly characterized inflammatory perturbation (*3, 4*). Care for trauma patients is complicated by multiple factors that affect clinical outcomes. First, while improvements in major hemorrhage protocols have saved lives, infusion of blood-derived products can lead to subsequent complications including coagulopathies(*5-9*). Second, tissue components released into circulation following trauma activate a non-specific inflammatory response(*10-13*). This inflammatory response is in part triggered by metabolic derangements initiated during initial tissue hypoxia and reperfusion(*14-19*). Finally, resuscitated and 'stabilized' patients are at risk of infection, in part due to a dysregulated inflammatory state that exhibits an attenuated response to invading pathogens(*10, 11*). Confounding this lack of knowledge of the endotypic milieu after trauma is the unknown prior health status of each individual patient and their specific responses to injury. Changes in hemostasis and inflammation, termed thromboinflammation, are central to this biology and have been characterized by our group and others(*20-25*). While significant advances over the preceding decades have saved lives, a broader understanding of how thromboinflammation drives patient-specific responses to shock and trauma is essential to provide personalized care for injured warfighters and civilians(*26, 27*).

While omics characterization has revolutionized cancer therapy and underlies personalized medicine, the care of the severely injured patient is based on overly simplified scoring systems, reductionist measures of a few mediators, or clinical "gestalt" which miss much of the existing post-injury biological dimensionality(*28-34*). Traditional clinical trials in trauma or associated sequalae have failed to provide sufficient insight and guidance to improve care(*35-40*).

Our group completed a randomized trial of plasma-based trauma resuscitation, which afforded a unique opportunity for controlled sampling, clinical care, and outcome data(*41*). We hypothesized that trans-omics profiling reveals underlying pathological differences in severely injured patients that may otherwise present with similar clinical profiles but ultimately have very different responses to treatment and clinical outcomes. Here, unsupervised clustering of molecular data obtained from severely injured patient plasma was performed to characterize untargeted metabolomics and proteomics signatures after trauma, and determine molecularly defined clinical trajectories and endotypes.

RESULTS

Trauma patient characteristics and data analysis workflow

A total of 97 healthy control subjects and 118 patients with both plasma metabolomics and proteomics were enrolled in this study (**Figure 1A**). Blood was collected at specified timepoints (Field, Emergency Department arrival (ED), post-injury hours 2, 4, 6, 12, 24, 48, 72, 120, 168) until the patient's discharge (**Figure 1B**), for a total of 856 samples (759 patient samples and 97 healthy controls). From patient plasma, 1012 proteins and 472 metabolites were quantified using untargeted DIA proteomics and metabolomics by liquid-chromatography coupled with tandem mass spectrometry (LC-MS/MS) (**Figure 1C**). Metabolomics and proteomics analyses were performed on these longitudinal samples, while clinical records were available for all patients throughout the study. Patients were grouped according to their shock severity (base excess (BE) at ED < -10 High Shock HS) and New Injury Severity Score (NISS) > 25 High Trauma HT) into High-Shock-High-Trauma (HSHT, N=35), High-Shock-Low-Trauma (HSLT, N=18), Low-Shock-High-Trauma (LSHT, N=28), and Low-Shock-Low-Trauma (LSLT, N=36) groups (**Figure**

1D). For 20 patients with missing BE at ED, omics data from an independent cohort of 333 trauma patients were employed to train and test an imputation model for value assignment (**Figure S1**). Patient characteristics have been previously detailed and are outlined here by S/T group (**Figure 1E**)(*41*). In this study, longitudinal omics trends were first analyzed in the 'average' trauma patient, and according to commonly used S/T grouping. Then, unsupervised hierarchical clustering of metabolomic and proteomic UMAP embeddings was performed to identify omics-based patient states and clinical patterns (**Figure 1F**). Finally, omics-based patient trajectories were identified according to their path through omics patient state space, yielding novel clinical and biological insight into trauma patient trajectories through injury and/or recovery (**Figure 1G**).

Omics patterns of the 'average' trauma patient

To analyze molecular patterns in the 'average' trauma patient, C-means clustering identified 10 unique, longitudinal kinetic patterns of omics data (**Figure S2**). For metabolomics we observed an early enrichment of the tricarboxylic acid (TCA) cycle and arginine biosynthesis, and prolonged amino acid and thiamine metabolism (**Figure 2A**, **Figure S3**). Hypotaurine and taurine metabolism peaked from 2-6 hours, and sphingolipid and histidine metabolism remained elevated until 24 hours. At 24-48 hours, we observed increases in plasma levels of nucleic acid, glutathione, and cyclic-ring amino acid metabolism; as well as hormone and fatty acid biosynthesis. Finally, 5-7 days post-injury had high levels of metabolites involved in biosynthesis of bile acids, aminoacyl-tRNA, proteolysis and amino acid metabolism.

For proteomics enrichment, there were initially high levels of proteins involved in detoxification, management of body fluid levels, and neutrophil and platelet degranulation (**Figure 2B, Figure S4**). This detoxification phase was followed by the initiation of a broad humoral

immune response, complement activation, and (regulation of) coagulation including clot formation and fibrinolysis. These proteins remained elevated out to ~24hrs, and were accompanied by a concomitant rise in protein-lipid (i.e. HDL) remodeling and lipid trafficking; an anti-microbial response, and a general response to wounding and hemostasis. From 24-48hrs there was a second spike in neutrophil degranulation proteins and an elevation in proteins involved in glycolysis and gluconeogenesis. Following this second spike was an acute phase response (APR), leukocyte adhesion and activity, negative regulation of complement, and a response to hypoxia.

For clinical measurements, consistent with the literature, we observed expected trends in clinical markers of shock, including early elevations in heart rate, lactate, and BE alongside reduced blood pressure that normalized quickly after resuscitation and hemorrhage control (**Figure 2C**). Additional measures of metabolic acidosis (pH, bicarbonate) were consistent with these trends as well. The average patient arrived coagulopathic with reduced MA and fibrinogen alongside elevated LY30 (clot lysis at 30 mins measured by thromboelastography (TEG)), which were also corrected over time, though not as abruptly as normalization in physiologic parameters of hemorrhagic shock. Patients arrived, on average, hypocalcemic with exacerbation of this hypocalcemia within the first 2 hours, secondary to the reported influx of calcium into the endothelium. Subsequent administration was likely responsible for the correction in ionized calcium.

Next, linear mixed modeling (adjusted for age, sex, shock/BE, injury/NISS, and time) was performed to identify proteins and metabolites highly associated with common clinical measurements (**Figure S5**). For metabolomics, strongest relationships were between carnitines and phosphates with platelet count, P_aO_2, and fibrinogen (**Figure 2D**); measures of hypoxia and fatty acid oxidation and vital signs; and between tissue injury metabolites (spermine, spermidine,

bilirubin, carnitines) and clotting. For proteomics, the strongest relationships were between clotting assays and coagulation and complement proteins; blood gas and APR proteins; and platelet count with complement and coagulation proteins (**Figure 2E**).

To assess the influence of the administration of pre-hospital plasma vs. saline, these groups were compared and significantly higher levels of CSF1R (macrophage colony stimulating factor receptor) and NAGLU (heparan sulfate degradation) were detected in patients treated with plasma products (**Figure S6**). There were no other protein or metabolite differences at any other timepoint, which is unsurprising due to the lack of clinical effect of prehospital plasma reported(*41*).

Analysis of omics by shock severity and tissue injury

Outcome for trauma patients is thought to be governed by a 'golden hour' where interventions within the first 60 minutes are deemed to be crucial to establishing a trajectory towards survival and good outcome. To identify metabolomic and proteomic expression patterns immediately following injury within this 'golden hour', patients were categorized by S/T scores (Figure 1D), and analyte levels were compared among these groups. A proteomic signature of tissue injury from significantly higher levels of 186 proteins was identified in the HT groups at ED (**Figure 3A**, **Figure S7**). Many of these were histones, extracellular (COL18A1, PRG4) or cytosolic (ACTAs, TUBBs, RHOA) proteins and are involved in cell metabolic processes (PSAT1, ARG1, ACAT2) or detoxification (ENO1, ADH, ALDH, SOD1) (**Figure 3B**). Significantly elevated proteins within the HS groups are primarily involved in antioxidant activity (FABP1, TXN, GSTA1) or glycolysis and gluconeogenesis (ALDOB, TPI1, LDHA) (**Figure 3C**). Beyond ED, HT patients had significantly elevated levels of glycolytic (ADH1B, GOT1, PGAM1), detoxification (FABP1, GSTA1, PRDX6, S100A9, CAT, CPN1), and tissue injury and hemolysis

proteins (MB, HBA, HBB) as well as decreased gelsolin (GSN) to bind circulating actin (**Figure 3D-G**). From 12-24 hours, within the HT groups were elevated levels of inflammatory proteins (SAA1/2, CRP, IL1RL1), peptidases and anti-microbials (CTSB, LBP, CHI3L1), as well as protease inhibitors (SERPINA1, TIMP1) and the tPA/fibrinolysis inhibitor SERPINE1. From 24-48 hours, HT groups also had significantly elevated fibrinogen chains (FGA, FGB, FGG), and decreased complement subunits (C1QB, C1QC).

For metabolomics, 37 metabolites were significantly elevated in the HSHT group (**Figure 3H**, **Figure S8**). Within HT, a wide range of metabolites including amino acids, nucleotides, galactose, and propanoate, as well as elevated levels of the hypoxic metabolite succinate and creatine (**Figure 3I**). In HS patients, there were significantly elevated levels of succinate, lactate, and polyamines as well as metabolites involved in the TCA cycle and beta-alanine and glycero(phospho)lipid metabolism (**Figure 3J**). Beyond ED, high levels of these metabolites persisted in the HSHT group until 6 hours, at which time the LSLT group showed elevated metabolites involved in biosynthesis of aminoacyl-tRNA, amino acids, and fatty acids indicating metabolic recovery (**Figure 3 K-N**).

HT patients frequently sustain traumatic brain injury (TBI) which complicates treatment and outcomes. For patients with TBI, proteomic differences in HSHT (elevated EXT2), LSHT (elevated SIGLEC14, PAICS, HPRT1, COMT; decreased ASGR2), or HT combined (CCL18 lymphocyte attraction) indicated differences in serum glycoprotein homeostasis, purine synthesis and metabolism, cell adhesion, and catecholamine degradation (**Figure S9**). Further, TBI patients within HT groups had consistently elevated levels of dopamine, and metabolites involved in (hypo)taurine metabolism and catecholamine biosynthesis.

Classification prediction and VIP analysis

Predicting the need for massive transfusion (MTX), and adverse outcomes including coagulopathy (International Normalized Ratio (INR) > 1.4), acute lung injury (ALI), extended ICU- (ICU-free days < median) and ventilator time (Vent-free days < median), and death can be difficult. Ensemble machine learning which creates an optimized, complied model was employed to predict outcomes and the need for MTX following trauma (model details in **Figure S10**)(*42*). Proteomic and metabolomics data collected at the ED timepoint were split into 75%-25% training and test sets, respectively. With AUC ~90% for death, coagulopathy, MTX, and ventilator time, and ~80% for ALI and ICU time, each outcome was associated with a unique panel of analytes contributing to Variable Importance in Projection (VIP) scores (**Figure 4**). With few exceptions, all the top VIP features were expressed at significantly higher levels in patients who experienced worse outcomes. Of note, both death and MTX VIPs indicated hypoxia, short-chain fatty acid metabolism, and elevated polyamines; INR VIPs indicated tissue and RBC lysis, and were involved in oxidative response; extended ICU stay, and extended ventilator VIPs enriched for glycolysis and high tissue oxidation, while ALI VIPs enriched for highly elevated catabolic processes, systemic inflammation, and RBC lysis. Further, models trained on an independent omics dataset of 333 trauma patients from a separate cohort (TACTIC study) predicted death (AUC 91%), ICU-free days (84%), and ventilator-free days (87%) in the COMBAT omic dataset (**Figure S11**).

Metabolic characterization of patient states from unsupervised clustering

Previously, unsupervised molecular clustering has been used to identify unique endotypes associated with differing outcomes within a broader patient population(*43-47*). Here, unsupervised clustering on Uniform Manifold Approximation and Projection (UMAP) embeddings of omics

data was employed to identify patient states based on metabolomics and proteomics profiles. Hierarchical clustering of 2D metabolomics UMAP embeddings yielded 8 distinct patient states as optimized by explained variance and power effect size analysis (**Figure 5A**, **Figure S12**). Datapoints associated with deaths, low ICU-free days, and severe injury (HSHT) were scattered across several patient states (PS 3, 5, 8. **Figure S12**). Two main metabolic meta states were observed and generally characterized by catabolism (Right), and energy production and biosynthesis (Left. **Figure 5A**. **Figure S13**). The density of datapoints per timepoint indicated the temporal nature of each patient state, with patient states classified as early injury (1, 5, 8), mid-injury (2, 3, 4), and late injury (6, 7) (**Figure 5B**). Differences in analyte expression revealed unique sets of metabolic pathways enriched in each patient state (**Figure 5C**, **Figure S14**). Patient state metabolomic signatures (median expression within the upper quartile) showed different longitudinal expression patterns indicating the nature of each state (**Figure 5C**, **Figure S14**). States 1 (lysophospholipids), 3 (pentose phosphate pathway), 5 (aromatic amino acids tryptophan and its indole derivative; tyrosine; branched chain and other amino acids – valine, citrulline; medium to long-chain acyl carnitines – AcCa 6:1, 18:0, 18:1; purine metabolites: hypoxanthine, urate, caffeine, theophylline; lysophosphatidyl-ethanolamines, -cholines and -serines of the 16:0 and 18:1; 20:4 C series) and 8 (markers of blood transfusion – mannitol and S-adenosylhomocysteine; antibiotics – amoxicilline) showed an enrichment at earlier time points, followed by progressive decline. Opposite trends were observed for states 2 (exogenous metabolites from iatrogenic intervention), 6 (carnitine metabolism and hemolysis markers) and 7 (pharmacological intervention with acetaminophen and pain management with opioids). Amino acid metabolism, especially sulfur amino acids, were over-represented in state 4 (cysteine, homocysteine,

kynurenine, leucine, methionine sulfoxide, phenylalanine, taurine), which showed no major temporal trends.

Clinically, each state expressed unique static and dynamic continuous clinical measurements associated with its omics signature (**Figure 5E-J**, **Figure S15**). For example, patient state 8 had the most perturbed vital signs (lowest body temperature and blood pressure), reflected the most shock (lowest BE and bicarbonate, highest lactate), and was the most coagulopathic (highest INR, lowest clotting factors). This state was further characterized by persistent brain injury (low GCS) and a longitudinal fibrinogenemic and thrombocytopenic coagulopathy. Other notable differences included those in blood chemistry (low P_aO_2 in state 4; low pH states 3 & 8), blood count (high WBCs, platelets, and hemoglobin and hematocrit in states 1, 2, 5), clotting (lowest PTT, INR, D-dimer in state 5; lowest Von Klauss fibrinogen in state 5), and transfusion of blood products (high tranexamic acid (TXA) in state 4; high RBCs, FFP, and crystalloids in states 4 & 8) (**Figure 5G-J**). Several states were clinically similar reflecting our hypothesis that metabolomic differences would distinguish otherwise clinically indistinguishable states.

Proteomics characterization of patient states from unsupervised clustering

For proteomics, hierarchical clustering of 2D UMAP embeddings also produced 8 distinct patient states (**Figure 6A**. **Figure S16**). Datapoints associated with death, low ICU-free days, and severe injury (HSHT) were more localized, clearly demarcating more severely (Right) and less severely-injured (Left) patient states (**Figure S16**). As with metabolomics, density of datapoints defined patient states to be associated with early- (states 1, 2, 7), mid- (3, 8), or late-injury (4, 5, 6) (**Figure 6B**). States 1 (early severe injury) and 3 (mid- severe injury) showed high levels of tissue injury proteins that enriched for catabolism, response to ROS, and neutrophil and platelet degranulation

(state 1), and proteasome expression, FA degradation, and response to stimuli in state 3 (**Figure 6B**, **C**. **Figure S17**). For later-injury states, state 4 had high levels of acute phase response (APR) proteins and early complement activation; while state 5 enriched for complement, cell adhesion, and acute inflammation. Other patient states contained less injured patient-timepoints and had higher levels of coagulation proteins such as F2 and F13B (states 2, 6, 8). State 7, an early injury cluster in between high injury state 1 and low injury state 2 had high levels of proteins involved in hemolysis and oxygen transport.

Clinically, states 1 and 3 had most perturbed vitals (lowest temp, blood pressure, GCS, and highest heart rate) and blood chemistry (lowest VCO_2, BE, bicarbonate; high lactate) (**Figure 6D-J**, **Figure S18**). These states also had coagulopathy and evidence of fibrinolysis (high PTT, INR, D-Dimer, TEGs; low clotting factors 7 and 9), and received high amounts of transfused blood products (RBCs, platelets, cryoprecipitate). States 2 (high P_aO_2, platelets, HGB, HCT, clotting factors; low body temp, D-Dimer), 7 (high P_aO_2, lactate; low body temp, clotting factors), and 8 (low heart rate, D-Dimer; high VCO_2) were mixed. The remaining states 4, 5, and 6 were clinically similar but had intermediate levels of clinical measurements operating at later timescales. Notable differences include SBP (high in states 4, 8; low in states 1, 5), D-dimer levels (low in states 2, 6, 8; high in states 1, 3, 4, 7), transfusion of FFP (high in states 1, 7), and pH (low in state 1, high in states 5, 6).

The combined metabolomics and proteomics model contained aspects of both models (**Figure S19**). Early severe injury state 4 had high levels of tissue injury proteins enriching for both metabolism and biosynthesis of organic molecules, response to stress, and neutrophil degranulation; and high levels of succinate, lactate (hypoxia), creatine, and carnitines. Late severe injury state 8 had high levels of analytes involved in glycolysis, gluconeogenesis, and

methylhistidine and pyruvate metabolism. Adjacent states 6 and 7 enriched for complement and coagulation cascades, acute phase response, bile acid synthesis, and fatty acid metabolism. Less sick patient states (1, 2, 3, 5) had high levels of taurine metabolism, complement proteins, glycolysis, fatty acid synthesis, and immunoglobulins.

Patient trajectories through metabolic patient states

To identify longitudinal trauma patient trajectories, patients were clustered according to their path through omic patient state UMAP space described above (Figure 7A). Dual multiple factor analysis was used to map each patient's omic data to a single point using a series of principal component normalization and reductions, similar in nature to patient-specific PCA analysis in identifying inflammatory endotypes (*45, 48*). Patients were then grouped by hierarchical clustering and their pathway through metabolomics-informed state space (**Figure S20**). Each trajectory had a unique signature of highly expressed metabolites that shifted dynamically across patient states over time (**Figure 7B**). Briefly, trajectories 2, 6, and 7 began with high tryptophan and methylhistidine metabolism (patient states 5, 8), markers of proteolysis, (muscle) tissue breakdown and catabolism(*49*). Trajectory 2 was short-lived, ending with high nicotinate and nicotinamide metabolism (**Figure 7B,C**), markers of NAD(P) breakdown. Patients in trajectory 6 transitioned to an increased metabolism of most substrates and most patients exited the study at ~24hours, while trajectory 7 patients ended with high levels of methylhistidine and FA metabolism and carnitine synthesis and stayed in the study out to 168 hrs. Patients in trajectory 4 began and ended with high (hypo)taurine and glutathione metabolism out to 168hr. Trajectory 1 began and ended mostly in state 1, was characterized by high aerobic glycolysis, and was short-lived (12hr). Patients in trajectories 3 and 5 also began in states of high glycolysis, transitioned to high thiamine,

riboflavin, and CoA metabolism, and metabolism of most substrates; and were both long-lived (168hr).

Clinically, there were no significant differences in ICU-free or Ventilator-free days, NISS, coagulopathy by INR, or incidences of TBI, ALI, or MTX (**Figure S21**). There were death-free trajectories (3, 4, 5) and trajectories with high incidences of blunt vs. penetrating injury although both were not significant. Trajectory 8, which began with high polyamine synthesis had a high heart rate, F11, and RBC transfusion; and low GCS and bicarbonate (**Figure 7D-E**, **Figure S21**). Additionally, only patients in this trajectory demonstrated high transition rates between the two meta-states of catabolism and biosynthesis. Trajectory 2 which began with high kynurenine biosynthesis and tissue injury, had clinically lower heart rate, body weight, GCS, von Clauss fibrinogen; and high fibrinolysis (ly30) and ended early (~12 hrs) with a high (29%) death rate (Figure 7D-N). Beginning in the same metabolic state was trajectory 6, with patients in this state shifting to polyamine biosynthesis and maintaining high levels of lactate and P_aO_2, and a lower heart rate and P_aCO_2. Trajectory 7 was similar but switched to the NAD salvage pathway, and was accompanied by lower lactate and a low D-Dimer and platelet count. Trajectory 4 uniquely began and remained in an energy and anti-oxidant biosynthesis metabolic state, and had a high heart rate, Von Clauss fibrinogen, transfusion with crystalloids, clotting F7; and low P_aO_2. Trajectory 1 began in the same state, but switched to an enriched TCA cycle state, and was accompanied by low fibrinogen and D-Dimer; and high HGB, HCT, and platelet count.

Patient trajectories through proteomic patient states

For proteomics, more severely- vs. less severely-injured, short- vs long-lived, and transitional trajectories were identified, each associated with unique proteomic signatures (**Figure 8A-C**,

Figure S22). Trajectories 1, 2, and 4 began in oxygen transport and clot stabilization states, and were short (6hr), medium (24hr), and long-lived (72-120hr), respectively (**Figure 8C**). Signatures for these trajectories enriched for hydrolase and peptidase activity and complement and coagulation cascades with high levels of IgGs and complement and coagulation proteins. Patients in trajectory 3 began with high levels of proteins involved in catabolism, degranulation, and oxidation; traveled through states of hemostasis, opsonization, and response to xenobiotics; and ended with high levels of complement, cell adhesion, and acute phase response proteins. Trajectory 5 was generalized by hemostasis, was long-lived (72-120hr), and also ended with high levels of complement and coagulation proteins. Trajectories 6, 7, and 8 represented patients with high transition among patient states (mainly between hemostasis and proteasome activation) and ending in complement activation and coagulation; and were short (6hr), medium (24hr), and long-lived (168hr) respectively. These trajectories enriched for adaptive immune response, phagocytosis, and fructose and aldehyde metabolism, respectively.

Clinically, trajectories 3 and 8 had the highest incidences of ALI, lung failure, liver failure, and heart failure (n.s.) (**Figure S23**). Interestingly trajectory 8 suffered predominately penetrating injuries and had no deaths, while 84% of trajectory 3 sustained blunt injuries. As with metabolomics, there were no significant differences in death, ventilator-free days, TBI, or MTX, and further there were no significant differences in BE among trajectories. Regarding other relevant outcomes, trajectory 8 had the lowest ICU-free days; and highest INR and days in the hospital. Further, trajectory 8 had high abdominal injury score and INR; low GCS, potassium, platelet count, HGB, and HCT, with this trajectory largely fluctuating between detoxification and hemostasis. Similarly, trajectory 3 had high NISS, Von Clauss fibrinogen, and D-Dimer; and low P_aO_2 and ly30. Beginning with clot formation and proteasome activation and ending with acute

phase response, trajectory 6 had pre-existing liver conditions and high BMI. Beginning with hemostasis, trajectory 1 had low hospital days, tissue injury, INR, Von Klauss fibrinogen, and D-Dimer; and high P_aCO_2, HCT, HGB, ly30 and ended with clot stabilization. Trajectory 2 began in a similar proteomic state and had low tissue injury and hospital days, but had high lactate and WBC and platelet count, ending with more complement activation and humoral immune response. Finally, trajectory 4 beginning with clot stabilization and ending with O_2 transport and hemostasis had high potassium, P_aO_2, platelet count, and PTT; and low HGB, HCT, and D-Dimer.

DISCUSSION

Clinicians rely on years of experience to gain the clinical acumen necessary to characterize the physiologic state of a patient, and predict the patients' likely clinical transition and outcome. While most wouldn't label it as such, treatment occurs in a Bayesian-like manner by considering the prior, perturbing the system via clinical management combined with clinical experience and scientific knowledge, and monitoring the change and clinical effectiveness in the next time iteration. This paradigm re-informs the prior and the process repeats as patients are hopefully guided toward recovery and away from death, significant morbidity, or complications. As more data becomes available, better clinical measurements and perturbations continue to narrow the confidence interval of a patient's given physiologic state. This will be accompanied by a more precise prediction of the patient's trajectory and what an effective treatment will be at a given time. Unfortunately, the trauma literature is filled with single and multivariate regression models and scoring systems, an approach that leads to overfit and misspecified models for outcome prediction. To remedy this gap, we here utilize longitudinal omics data to provide a more comprehensive characterization of the post-trauma response to injury and subsequent treatment. These findings

provide a more holistic/global view of the post trauma-milieu, and most importantly reveal that patients separate into biologic phenotypes which cannot be discerned by demographic, injury, or clinical data.

We report distinct metabolomics- and proteomics-informed trauma patient states and trajectories. In doing so we characterized injured patients via their underlying biology rather than their demographic or physiologic readouts. This allowed for an agnostic characterization in line with our clinical conjecture that patients often have similar demographic, injury or physiologic traits yet seemingly different underlying biology, responses to injury and treatment, and resultant outcomes. Indeed, while there are some clinical differences which may be identifiable to the astute clinician, most of these endotypes and trajectories are based on molecular omics signatures. Taken together these data indicate that patients can fall under multiple endotypes of metabolic energy crisis, coagulopathies, complement activation and dysfunctional thromboinflammation. As expected, these states are dynamic and transition as the patients do based on response to injury, resuscitation and treatment. We thus determined trajectories comprised of those states which reflect dynamic signatures that are not necessarily distinguishable by clinical characteristics. This novel finding helps to explain the clinical observation of multiple clinically identical patients with divergent responses to injury, resuscitation, and divergent outcomes.

We expect molecular-based trajectory data like these –when optimized, to augment our current patient classification, and outcome prediction. For example, there were no significant differences in BE upon arrival or NISS among trajectories, yet trajectories 1 and 2 had relatively high mortality rates (24%, 29%) compared to others. Further, trajectories 2, 6, and 7 begin with similar metabolic starting points of high kynurenine and methylhistidine synthesis (tissue injury). Trajectory 2 is relatively short-lived with a high mortality rate, while 6/7 are long-lived and are

accompanied by metabolic shifts to purine metabolism/NAD salvage respectively as well as clinical differences in clotting factors, blood gas and blood composition (hematocrit, hemoglobin, platelet count), and vitals (heart rate and body weight). For proteomics, trajectory 8 had significantly elevated INR and hospital stay, and lower ICU-free days despite no significant differences in BE or NISS (although elevated). Additionally, trajectories 5 and 6 both share similar clinical measurements but 5 shift to acute phase response and proteasome activation while 6 stays in detoxification and hemostasis states. We expect that for direct applicability to the clinic, a rapid means of quick state identification and transition propensity can be employed from similar work. This would allow for phenotypes based on omics endotypes to provide prediction and decision support based on multivariate data which would otherwise be too complicated to discern. This then is a more formalistic modeling of experienced clinician gestalt. Future work to refine, rapidly identify states via quick (perhaps targeted field) measurement (with portable devices), dimension reduction, trajectory tracking and prediction is planned and essential to realize the goal of personalized omics for the dual goal of identifying intervenable mechanistic pathways and guiding individual treatment toward the unified goal of saving lives.

Previously, several groups have reported on the use of omics signatures to phenotype after trauma. The Glue Grant utilized then novel technologies to assay gene expression after trauma, and was revolutionary for showing a genomic storm with an estimated ~80% of the genome disturbed following trauma (*50, 51*). Unfortunately, the durability of the Glue Grant findings was hampered by methodologic concerns including sample timing, which was taken at nonstandard intervals over a long period of time after injury. In addition, while there were a small number of individual metabolites assayed the technology was not sufficiently advanced and only evaluated gene expression with no evaluation of proteomic and metabolomic changes. Most recently several

groups have reported characterization of gene expression, and trans-omic changes after trauma. These analyses include test and training set clustered prediction modeling and evaluation of endotypes related to beneficial outcome from the PAMPer trial(*47*). These advances in omics (proteomics, metabolomics) studies have allowed for readouts closer to patient phenotype. However, to date, they have not been used to identify unsupervised molecular patient states and trajectories. Our group and others have utilized longitudinal multivariate biomarker data to characterize illness and injury, have shown effective prediction of outcomes, and garnered biologic pathway insight(*42-47, 52-71*). Inspired by this work, here we identified unique endotypes and trajectories that can be guided or annotated through clinical supervision. It is identification of these endotypes and trajectories which makes this analysis most unique, and allows us to use clinical knowledge and context to ascertain their meaning. Future work will center around codifying and clinically understanding the drivers of these discrete trajectories with the ultimate goal of rapid point of care precision medicine guided by state and trajectory identification. This therefore would allow for tailored treatment and clinical guidance of trajectories towards recovery.

Limitations with this study include sample size and sparsity in some outcomes (mortality). While sample collection was very good for this study there is some natural missingness of measurements based on censoring (death or discharge) and random missingness due to the occasional inability to collect some clinical samples due to logistics and priority of treatment in the harried nature of trauma care. Because of this we further understand that this can negatively impact our model outputs. We have attempted to mitigate this with cross validation with an independent cohort of patients as described in the methods. Furthermore, we believe the novelty of this work is the ability to clinically and biologically supervise our results giving clinical context

to the model outputs. We expect that future studies and resulting data will mitigate and allow for testing and refinement of our models.

MATERIALS AND METHODS

See Supplementary files for extended methods

Experimental design: The overall hypothesis for this observational study was that plasma omics data will give new insights into trauma patient classification, endotypes, and clinical outcome prediction. The objectives of this study were 1) to identify standard S/T omics signatures; and 2) identify trauma patient omics endotypes and trajectories. All patients enrolled in COMBAT with both metabolomic and proteomic data available were included, totaling 118 patients and 97 healthy controls, and none were treated as outliers. Plasma underwent LC-MS/MS proteomics and metabolomics. Blood was used to measure biochemical and coagulation data using standard clinical measurements, viscoelastic hemostatic assays, coagulation factor levels, and cytokine and chemokine levels using ELISA. Endpoints for the study were 168 hours post-injury, or the final timepoint of hospital care regardless of discharge status. For biological and technical replicates, N=1 plasma samples were collected from each patient at each timepoint.

Proteomics: Plasma samples were digested in an S-Trap 96-well plate using trypsin. Peptide solutions were pooled, lyophilized, resuspended in 0.1% formic acid, and loaded onto Evotips. Peptides were separated using the Evosep One system coupled to the timsTOF Pro mass spectrometer (diaPASEF mode) via the nano-electrospray ion source. M/Z spectra were searched in Spectronaut, and data are presented as units of relative intensity.

Ultra-High-Pressure Liquid Chromatography-Mass Spectrometry metabolomics: Frozen plasma aliquots (10 µL) were extracted 1:25 in ice cold extraction solution (methanol:acetonitrile:water 5:3:2 v/v/v). Samples were vortexed for 30 min at 4°C, prior to centrifugation for 10 min at 15,000g at 4°C. Analyses were performed using a Vanquish UHPLC coupled online to a Q Exactive mass spectrometer (ThermoFisher). Samples were analyzed using a 1 min and 5 minute gradient-based method, spectra were searched in Maven, and data are presented as units of relative intensity.

Bioinformatics and data processing: Omics variables with constant values were removed, and values at or below the limit of detection were imputed with 20% the minimum value for that analyte. R software and packages (versions and citations in supplemental files) were used for data analysis and generating all graphs. Mfuzz was used for C-means clustering, EnhancedVolcano created volcano plots, and pheatmap generated heatmaps. UMAP was used to create a 2D embedding of the omic manifold, followed by hierarchical clustering to identify patient states. Dual multiple factor analysis was employed on embeddings for hierarchical clustering to identify patient trajectories. The number of clusters was chosen using a combination of percent of variance explained, power effect size (η^2), the gap statistic, and silhouette method. Metaboanalyst and Metascape were used for pathway enrichment.

Statistical analysis: Data were log2-transformed to approximate and assume normal distribution for statistical analyses (**Figure S24**). Significant differences were determined as $P<0.05$ using one-way ANOVA with TukeyHSD post-hoc analysis, Student's t-test, or Pearson Chi-squared test. Omic comparisons were corrected using the Benjamini-Hochberg FDR method, and shown with median +/- IQR in boxplots or median +/- SEM in timeseries line graphs. Continuous clinical data

with $P < 0.05$ was considered statistically significant, and shown using median +/- IQR. Linear mixed modeling was used to determine associations between analytes and clinical measurements (fixed effects age, sex, and time; random effects S/T group, individual patient); and to identify analytes and clinical measurements that had significant interactions with time per group (group*time; random effect of individual patient). Sidak post-hoc correction was performed on the estimated marginal means of mixed models. The partial slope was used as the primary measurement and for visualization in the circus plots. Ensemble methods for classification were built using SuperLearner with full details in SF10, receiver operating characteristic curves were calculated to show model performance using the area under the curve, and VIP of analytes were calculated using 5x repeated 5-fold cross-validation with RandomForest.

REFERENCES

1. R. A. Callcut, L. Z. Kornblith, A. S. Conroy, A. J. Robles, J. P. Meizoso, N. Namias, D. E. Meyer, A. Haymaker, M. S. Truitt, V. Agrawal, J. M. Haan, K. L. Lightwine, J. M. Porter, J. L. San Roman, W. L. Biffl, M. S. Hayashi, M. J. Sise, J. Badiee, G. Recinos, K. Inaba, T. J. Schroeppel, E. Callaghan, J. A. Dunn, S. Godin, R. C. McIntyre, Jr., E. D. Peltz, P. J. O'Neill, C. F. Diven, A. M. Scifres, E. E. Switzer, M. A. West, S. Storrs, D. C. Cullinane, J. F. Cordova, E. E. Moore, H. B. Moore, A. R. Privette, E. A. Eriksson, M. J. Cohen, The why and how our trauma patients die: A prospective Multicenter Western Trauma Association study. *J Trauma Acute Care Surg* **86**, 864-870 (2019).
2. E. Gonzalez, E. E. Moore, H. B. Moore, M. P. Chapman, T. L. Chin, A. Ghasabyan, M. V. Wohlauer, C. C. Barnett, D. D. Bensard, W. L. Biffl, C. C. Burlew, J. L. Johnson, F. M. Pieracci, G. J. Jurkovich, A. Banerjee, C. C. Silliman, A. Sauaia, Goal-directed Hemostatic Resuscitation of Trauma-induced Coagulopathy: A Pragmatic Randomized Clinical Trial Comparing a Viscoelastic Assay to Conventional Coagulation Assays. *Ann Surg* **263**, 1051-1059 (2016).
3. J. M. Lord, M. J. Midwinter, Y. F. Chen, A. Belli, K. Brohi, E. J. Kovacs, L. Koenderman, P. Kubes, R. J. Lilford, The systemic immune response to trauma: an overview of pathophysiology and treatment. *Lancet (London, England)* **384**, 1455-1465 (2014).
4. R. C. Bone, Toward an Epidemiology and Natural History of SIRS (Systemic Inflammatory Response Syndrome). *JAMA* **268**, 3452-3455 (1992).

5. E. E. Moore, H. B. Moore, L. Z. Kornblith, M. D. Neal, M. Hoffman, N. J. Mutch, H. Schöchl, B. J. Hunt, A. Sauaia, Trauma-induced coagulopathy. *Nat Rev Dis Primers* **7**, 30 (2021).
6. J. W. Cannon, M. A. Khan, A. S. Raja, M. J. Cohen, J. J. Como, B. A. Cotton, J. J. Dubose, E. E. Fox, K. Inaba, C. J. Rodriguez, J. B. Holcomb, J. C. Duchesne, Damage control resuscitation in patients with severe traumatic hemorrhage: A practice management guideline from the Eastern Association for the Surgery of Trauma. *J Trauma Acute Care Surg* **82**, 605-617 (2017).
7. R. L. Gruen, K. Brohi, M. Schreiber, Z. J. Balogh, V. Pitt, M. Narayan, R. V. Maier, Haemorrhage control in severely injured patients. *The Lancet* **380**, 1099-1108 (2012).
8. J. B. Holcomb, D. Jenkins, P. Rhee, J. Johannigman, P. Mahoney, S. Mehta, E. D. Cox, M. J. Gehrke, G. J. Beilman, M. Schreiber, Damage control resuscitation: directly addressing the early coagulopathy of trauma. *Journal of Trauma and Acute Care Surgery* **62**, 307-310 (2007).
9. P. I. Johansson, R. S. Oliveri, S. R. Ostrowski, Hemostatic resuscitation with plasma and platelets in trauma. *J Emerg Trauma Shock* **5**, 120-125 (2012).
10. J. M. Lord, M. J. Midwinter, Y.-F. Chen, A. Belli, K. Brohi, E. J. Kovacs, L. Koenderman, P. Kubes, R. J. Lilford, The systemic immune response to trauma: an overview of pathophysiology and treatment. *The Lancet* **384**, 1455-1465 (2014).
11. R. C. Bone, Sir Isaac Newton, sepsis, SIRS, and CARS. *Crit Care Med* **24**, 1125-1128 (1996).
12. K.-M. Kaukonen, M. Bailey, D. Pilcher, D. J. Cooper, R. Bellomo, Systemic inflammatory response syndrome criteria in defining severe sepsis. *New England Journal of Medicine* **372**, 1629-1638 (2015).
13. A. Komori, H. Iriyama, T. Kainoh, M. Aoki, T. Naito, T. Abe, The impact of infection complications after trauma differs according to trauma severity. *Scientific reports* **11**, 1-8 (2021).
14. N. Clendenen, G. R. Nunns, E. E. Moore, J. A. Reisz, E. Gonzalez, E. Peltz, C. C. Silliman, M. Fragoso, T. Nemkov, M. J. Wither, K. Hansen, A. Banerjee, H. B. Moore, A. D'Alessandro, Hemorrhagic shock and tissue injury drive distinct plasma metabolome derangements in swine. *The journal of trauma and acute care surgery* **83**, 635-642 (2017).
15. A. D'Alessandro, A. L. Slaughter, E. D. Peltz, E. E. Moore, C. C. Silliman, M. Wither, T. Nemkov, A. W. Bacon, M. Fragoso, A. Banerjee, K. C. Hansen, Trauma/hemorrhagic shock instigates aberrant metabolic flux through glycolytic pathways, as revealed by preliminary (13)C-glucose labeling metabolomics. *Journal of translational medicine* **13**, 253 (2015).
16. A. D'alessandro, H. B. Moore, E. E. Moore, M. Wither, T. Nemkov, E. Gonzalez, A. Slaughter, M. Fragoso, K. C. Hansen, C. C. Silliman, Early hemorrhage triggers metabolic responses that build up during prolonged shock. *American Journal of Physiology-Regulatory, Integrative and Comparative Physiology* **308**, R1034-R1044 (2015).
17. A. L. Slaughter, A. D'Alessandro, E. E. Moore, A. Banerjee, C. C. Silliman, K. C. Hansen, J. A. Reisz, M. Fragoso, M. J. Wither, A. W. Bacon, H. B. Moore, E. D. Peltz, Glutamine metabolism drives succinate accumulation in plasma and the lung during hemorrhagic shock. *J Trauma Acute Care Surg* **81**, 1012-1019 (2016).

18. A. D'Alessandro, T. Nemkov, H. B. Moore, E. E. Moore, M. Wither, T. Nydam, A. Slaughter, C. C. Silliman, A. Banerjee, K. C. Hansen, Metabolomics of trauma-associated death: shared and fluid-specific features of human plasma vs lymph. *Blood Transfusion* **14**, 185 (2016).
19. E. D. Peltz, A. D'Alessandro, E. E. Moore, T. Chin, C. C. Silliman, A. Sauaia, K. C. Hansen, A. Banerjee, Pathologic metabolism: an exploratory study of the plasma metabolome of critical injury. *The journal of trauma and acute care surgery* **78**, 742 (2015).
20. S. P. Jackson, R. Darbousset, S. M. Schoenwaelder, Thromboinflammation: challenges of therapeutically targeting coagulation and other host defense mechanisms. *Blood* **133**, 906-918 (2019).
21. M. DeBot, C. Erickson, M. Kelher, T. R. Schaid, Jr., E. E. Moore, A. Sauaia, A. Cralley, I. LaCroix, A. D'Alessandro, K. Hansen, M. J. Cohen, C. C. Silliman, J. Coleman, Platelet and cryoprecipitate transfusions from female donors improve coagulopathy in vitro. *J Trauma Acute Care Surg* **94**, 497-503 (2023).
22. T. R. Schaid, Jr., K. C. Hansen, A. Sauaia, E. E. Moore, M. DeBot, A. L. Cralley, C. Erickson, C. C. Silliman, A. Banerjee, A. Ghasabyan, K. Jones, I. Lacroix, S. Mitra, A. D'Alessandro, M. J. Cohen, Postinjury complement C4 activation is associated with adverse outcomes and is potentially influenced by plasma resuscitation. *J Trauma Acute Care Surg* **93**, 588-596 (2022).
23. A. P. Eitel, E. E. Moore, A. Sauaia, M. R. Kelher, N. G. Vigneshwar, M. G. Bartley, J. B. Hadley, C. C. Burlew, E. M. Campion, C. J. Fox, R. A. Lawless, F. M. Pieracci, K. B. Platnick, H. B. Moore, M. J. Cohen, C. C. Silliman, A proposed clinical coagulation score for research in trauma-induced coagulopathy. *J Trauma Acute Care Surg* **94**, 798-802 (2023).
24. M. DeBot, A. P. Eitel, E. E. Moore, A. Sauaia, P. Lutz, T. R. Schaid, Jr., J. B. Hadley, D. J. Kissau, M. J. Cohen, M. R. Kelher, C. C. Silliman, BLOOD TYPE O IS A RISK FACTOR FOR HYPERFIBRINOLYSIS AND MASSIVE TRANSFUSION AFTER SEVERE INJURY. *Shock* **58**, 492-497 (2022).
25. J. R. Coleman, E. E. Moore, M. R. Kelher, K. Jones, M. J. Cohen, A. Banerjee, C. C. Silliman, Elucidating the molecular mechanisms of fibrinolytic shutdown after severe injury: The role of thrombin-activatable fibrinolysis inhibitor. *J Trauma Acute Care Surg* **94**, 857-862 (2023).
26. R. Norton, O. Kobusingye, Injuries. *New England Journal of Medicine* **368**, 1723-1730 (2013).
27. E. J. MacKenzie, F. P. Rivara, G. J. Jurkovich, A. B. Nathens, K. P. Frey, B. L. Egleston, D. S. Salkever, D. O. Scharfstein, A national evaluation of the effect of trauma-center care on mortality. *The New England journal of medicine* **354**, 366-378 (2006).
28. R. Chen, G. I. Mias, J. Li-Pook-Than, L. Jiang, H. Y. Lam, R. Chen, E. Miriami, K. J. Karczewski, M. Hariharan, F. E. Dewey, Y. Cheng, M. J. Clark, H. Im, L. Habegger, S. Balasubramanian, M. O'Huallachain, J. T. Dudley, S. Hillenmeyer, R. Haraksingh, D. Sharon, G. Euskirchen, P. Lacroute, K. Bettinger, A. P. Boyle, M. Kasowski, F. Grubert, S. Seki, M. Garcia, M. Whirl-Carrillo, M. Gallardo, M. A. Blasco, P. L. Greenberg, P. Snyder, T. E. Klein, R. B. Altman, A. J. Butte, E. A. Ashley, M. Gerstein, K. C. Nadeau, H. Tang, M. Snyder, Personal omics profiling reveals dynamic molecular and medical phenotypes. *Cell* **148**, 1293-1307 (2012).

29. Y. Hasin, M. Seldin, A. Lusis, Multi-omics approaches to disease. *Genome Biology* **18**, 83 (2017).
30. K. J. Karczewski, M. P. Snyder, Integrative omics for health and disease. *Nature Reviews Genetics* **19**, 299-310 (2018).
31. S. M. Schüssler-Fiorenza Rose, K. Contrepois, K. J. Moneghetti, W. Zhou, T. Mishra, S. Mataraso, O. Dagan-Rosenfeld, A. B. Ganz, J. Dunn, D. Hornburg, S. Rego, D. Perelman, S. Ahadi, M. R. Sailani, Y. Zhou, S. R. Leopold, J. Chen, M. Ashland, J. W. Christle, M. Avina, P. Limcaoco, C. Ruiz, M. Tan, A. J. Butte, G. M. Weinstock, G. M. Slavich, E. Sodergren, T. L. McLaughlin, F. Haddad, M. P. Snyder, A longitudinal big data approach for precision health. *Nature Medicine* **25**, 792-804 (2019).
32. M. Chun, Y. Zhang, C. Becnel, T. Brown, M. Hussein, E. Toraih, S. Taghavi, C. Guidry, J. Duchesne, R. Schroll, P. McGrew, New Injury Severity Score and Trauma Injury Severity Score are superior in predicting trauma mortality. *Journal of Trauma and Acute Care Surgery* **92**, 528-534 (2022).
33. J. Qi, L. Bao, P. Yang, D. Chen, Comparison of base excess, lactate and pH predicting 72-h mortality of multiple trauma. *BMC Emergency Medicine* **21**, 1-7 (2021).
34. A. Schork, K. Moll, M. Haap, R. Riessen, R. Wagner, Course of lactate, pH and base excess for prediction of mortality in medical intensive care patients. *PloS one* **16**, e0261564 (2021).
35. K. Baksaas-Aasen, L. S. Gall, J. Stensballe, N. P. Juffermans, N. Curry, M. Maegele, A. Brooks, C. Rourke, S. Gillespie, J. Murphy, R. Maroni, P. Vulliamy, H. H. Henriksen, K. H. Pedersen, K. M. Kolstadbraaten, M. R. Wirtz, D. J. B. Kleinveld, N. Schäfer, S. Chinna, R. A. Davenport, P. A. Naess, J. C. Goslings, S. Eaglestone, S. Stanworth, P. I. Johansson, C. Gaarder, K. Brohi, Viscoelastic haemostatic assay augmented protocols for major trauma haemorrhage (ITACTIC): a randomized, controlled trial. *Intensive Care Med* **47**, 49-59 (2021).
36. J. B. Holcomb, B. C. Tilley, S. Baraniuk, E. E. Fox, C. E. Wade, J. M. Podbielski, D. J. del Junco, K. J. Brasel, E. M. Bulger, R. A. Callcut, M. J. Cohen, B. A. Cotton, T. C. Fabian, K. Inaba, J. D. Kerby, P. Muskat, T. O'Keeffe, S. Rizoli, B. R. H. Robinson, T. M. Scalea, M. A. Schreiber, D. M. Stein, J. A. Weinberg, J. L. Callum, J. R. Hess, N. Matijevic, C. N. Miller, J.-F. Pittet, D. B. Hoyt, G. D. Pearson, B. Leroux, G. van Belle, f. t. P. S. Group, Transfusion of Plasma, Platelets, and Red Blood Cells in a 1:1:1 vs a 1:1:2 Ratio and Mortality in Patients With Severe Trauma: The PROPPR Randomized Clinical Trial. *JAMA* **313**, 471-482 (2015).
37. F. X. Guyette, J. B. Brown, M. S. Zenati, B. J. Early-Young, P. W. Adams, B. J. Eastridge, R. Nirula, G. A. Vercruysse, T. O'Keeffe, B. Joseph, L. H. Alarcon, C. W. Callaway, B. S. Zuckerbraun, M. D. Neal, R. M. Forsythe, M. R. Rosengart, T. R. Billiar, D. M. Yealy, A. B. Peitzman, J. L. Sperry, S. S. Group, Tranexamic Acid During Prehospital Transport in Patients at Risk for Hemorrhage After Injury: A Double-blind, Placebo-Controlled, Randomized Clinical Trial. *JAMA Surgery* **156**, 11-20 (2021).
38. A. C. Gordon, A. J. Mason, N. Thirunavukkarasu, G. D. Perkins, M. Cecconi, M. Cepkova, D. G. Pogson, H. D. Aya, A. Anjum, G. J. Frazier, Effect of early vasopressin vs norepinephrine on kidney failure in patients with septic shock: the VANISH randomized clinical trial. *Jama* **316**, 509-518 (2016).

39. D. F. McAuley, J. G. Laffey, C. M. O'Kane, G. D. Perkins, B. Mullan, T. J. Trinder, P. Johnston, P. A. Hopkins, A. J. Johnston, C. McDowell, Simvastatin in the acute respiratory distress syndrome. *New England Journal of Medicine* **371**, 1695-1703 (2014).
40. J. B. Holcomb, D. J. del Junco, E. E. Fox, C. E. Wade, M. J. Cohen, M. A. Schreiber, L. H. Alarcon, Y. Bai, K. J. Brasel, E. M. Bulger, B. A. Cotton, N. Matijevic, P. Muskat, J. G. Myers, H. A. Phelan, C. E. White, J. Zhang, M. H. Rahbar, f. t. PROMMTT Study Group, The Prospective, Observational, Multicenter, Major Trauma Transfusion (PROMMTT) Study: Comparative Effectiveness of a Time-Varying Treatment With Competing Risks. *JAMA Surgery* **148**, 127-136 (2013).
41. H. B. Moore, E. E. Moore, M. P. Chapman, K. McVaney, G. Bryskiewicz, R. Blechar, T. Chin, C. C. Burlew, F. Pieracci, F. B. West, Plasma-first resuscitation to treat haemorrhagic shock during emergency ground transportation in an urban area: a randomised trial. *The Lancet* **392**, 283-291 (2018).
42. A. D. Grossman, M. J. Cohen, G. T. Manley, A. J. Butte, Altering physiological networks using drugs: steps towards personalized physiology. *BMC Med Genomics* **6 Suppl 2**, S7 (2013).
43. M. R. Thau, T. Liu, N. A. Sathe, G. E. O'Keefe, B. R. H. Robinson, E. Bulger, C. E. Wade, E. E. Fox, J. B. Holcomb, W. C. Liles, I. B. Stanaway, C. Mikacenic, M. M. Wurfel, P. K. Bhatraju, E. D. Morrell, Association of Trauma Molecular Endotypes With Differential Response to Transfusion Resuscitation Strategies. *JAMA Surg*, (2023).
44. C. A. I. Åkerlund, A. Holst, N. Stocchetti, E. W. Steyerberg, D. K. Menon, A. Ercole, D. W. Nelson, Clustering identifies endotypes of traumatic brain injury in an intensive care cohort: a CENTER-TBI study. *Crit Care* **26**, 228 (2022).
45. L. Schimunek, H. Lindberg, M. Cohen, R. A. Namas, Q. Mi, J. Yin, D. Barclay, F. El-Dehaibi, A. Abboud, R. Zamora, T. R. Billiar, Y. Vodovotz, Computational Derivation of Core, Dynamic Human Blunt Trauma Inflammatory Endotypes. *Front Immunol* **11**, 589304 (2020).
46. S. C. Brakenridge, Z. Wang, M. Cox, S. Raymond, R. Hawkins, D. Darden, G. Ghita, B. Brumback, J. Cuschieri, R. V. Maier, F. A. Moore, A. M. Mohr, P. A. Efron, L. L. Moldawer, Distinct immunologic endotypes are associated with clinical trajectory after severe blunt trauma and hemorrhagic shock. *J Trauma Acute Care Surg* **90**, 257-267 (2021).
47. J. Wu, Y. Vodovotz, S. Abdelhamid, F. X. Guyette, M. B. Yaffe, D. S. Gruen, A. Cyr, D. O. Okonkwo, U. K. Kar, N. Krishnamoorthi, R. G. Voinchet, I. M. Billiar, M. H. Yazer, R. A. Namas, B. J. Daley, R. S. Miller, B. G. Harbrecht, J. A. Claridge, H. A. Phelan, B. S. Zuckerbraun, P. I. Johansson, J. Stensballe, J. H. Morrissey, R. P. Tracy, S. R. Wisniewski, M. D. Neal, J. L. Sperry, T. R. Billiar, Multi-omic analysis in injured humans: Patterns align with outcomes and treatment responses. *Cell Rep Med* **2**, 100478 (2021).
48. H. Abdi, L. J. Williams, D. Valentin, Multiple factor analysis: principal component analysis for multitable and multiblock data sets. *Wiley Interdisciplinary reviews: computational statistics* **5**, 149-179 (2013).
49. S. A. Rice, G. A. Ten Have, J. A. Reisz, S. Gehrke, D. Stefanoni, C. Frare, Z. Barati, R. H. Coker, A. D'Alessandro, N. E. Deutz, Nitrogen recycling buffers against ammonia toxicity from skeletal muscle breakdown in hibernating arctic ground squirrels. *Nature metabolism* **2**, 1459-1471 (2020).

50. S. E. Calvano, W. Xiao, D. R. Richards, R. M. Felciano, H. V. Baker, R. J. Cho, R. O. Chen, B. H. Brownstein, J. P. Cobb, S. K. Tschoeke, C. Miller-Graziano, L. L. Moldawer, M. N. Mindrinos, R. W. Davis, R. G. Tompkins, S. F. Lowry, A network-based analysis of systemic inflammation in humans. *Nature* **437**, 1032-1037 (2005).
51. R. G. Tompkins, Genomics of injury: The Glue Grant experience. *J Trauma Acute Care Surg* **78**, 671-686 (2015).
52. P. K. Bhatraju, L. R. Zelnick, J. Herting, R. Katz, C. Mikacenic, S. Kosamo, E. D. Morrell, C. Robinson-Cohen, C. S. Calfee, J. D. Christie, K. D. Liu, M. A. Matthay, W. O. Hahn, V. Dmyterko, N. S. J. Slivinski, J. A. Russell, K. R. Walley, D. C. Christiani, W. C. Liles, J. Himmelfarb, M. M. Wurfel, Identification of Acute Kidney Injury Subphenotypes with Differing Molecular Signatures and Responses to Vasopressin Therapy. *Am J Respir Crit Care Med* **199**, 863-872 (2019).
53. K. R. Famous, K. Delucchi, L. B. Ware, K. N. Kangelaris, K. D. Liu, B. T. Thompson, C. S. Calfee, Acute Respiratory Distress Syndrome Subphenotypes Respond Differently to Randomized Fluid Management Strategy. *Am J Respir Crit Care Med* **195**, 331-338 (2017).
54. C. W. Seymour, J. N. Kennedy, S. Wang, C.-C. H. Chang, C. F. Elliott, Z. Xu, S. Berry, G. Clermont, G. Cooper, H. Gomez, Derivation, validation, and potential treatment implications of novel clinical phenotypes for sepsis. *Jama* **321**, 2003-2017 (2019).
55. R. A. Namas, Y. Vodovotz, K. Almahmoud, O. Abdul-Malak, A. Zaaqoq, R. Namas, Q. Mi, D. Barclay, B. Zuckerbraun, A. B. Peitzman, Temporal patterns of circulating inflammation biomarker networks differentiate susceptibility to nosocomial infection following blunt trauma in humans. *Annals of surgery* **263**, 191 (2016).
56. A. Cyr, Y. Zhong, S. E. Reis, R. A. Namas, A. Amoscato, B. Zuckerbraun, J. Sperry, R. Zamora, Y. Vodovotz, T. R. Billiar, Analysis of the Plasma Metabolome after Trauma, Novel Circulating Sphingolipid Signatures, and In-Hospital Outcomes. *J Am Coll Surg* **232**, 276-287.e271 (2021).
57. S. R. Li, F. Guyette, J. Brown, M. Zenati, K. M. Reitz, B. Eastridge, R. Nirula, G. A. Vercruysse, T. O'Keeffe, B. Joseph, M. D. Neal, B. S. Zuckerbraun, J. L. Sperry, Early Prehospital Tranexamic Acid Following Injury Is Associated With a 30-day Survival Benefit: A Secondary Analysis of a Randomized Clinical Trial. *Ann Surg* **274**, 419-426 (2021).
58. Effects of tranexamic acid on death, vascular occlusive events, and blood transfusion in trauma patients with significant haemorrhage (CRASH-2): a randomised, placebo-controlled trial. *The Lancet* **376**, 23-32 (2010).
59. J. L. Sperry, F. X. Guyette, J. B. Brown, M. H. Yazer, D. J. Triulzi, B. J. Early-Young, P. W. Adams, B. J. Daley, R. S. Miller, B. G. Harbrecht, Prehospital plasma during air medical transport in trauma patients at risk for hemorrhagic shock. *New England Journal of Medicine* **379**, 315-326 (2018).
60. H. A. Ladhani, V. P. Ho, C. C. Charbonnet, J. L. Sperry, F. X. Guyette, J. B. Brown, B. J. Daley, R. S. Miller, B. G. Harbrecht, H. A. Phelan, J. A. Claridge, Dose-dependent association between blood transfusion and nosocomial infections in trauma patients: A secondary analysis of patients from the PAMPer trial. *J Trauma Acute Care Surg* **91**, 272-278 (2021).

61. C. S. Calfee, K. Delucchi, P. E. Parsons, B. T. Thompson, L. B. Ware, M. A. Matthay, Subphenotypes in acute respiratory distress syndrome: latent class analysis of data from two randomised controlled trials. *The Lancet Respiratory Medicine* **2**, 611-620 (2014).
62. A. E. Pusateri, E. E. Moore, H. B. Moore, T. D. Le, F. X. Guyette, M. P. Chapman, A. Sauaia, A. Ghasabyan, J. Chandler, K. McVaney, J. B. Brown, B. J. Daley, R. S. Miller, B. G. Harbrecht, J. A. Claridge, H. A. Phelan, W. R. Witham, A. T. Putnam, J. L. Sperry, Association of Prehospital Plasma Transfusion With Survival in Trauma Patients With Hemorrhagic Shock When Transport Times Are Longer Than 20 Minutes: A Post Hoc Analysis of the PAMPer and COMBAT Clinical Trials. *JAMA Surgery* **155**, e195085-e195085 (2020).
63. D. B. Antcliffe, K. L. Burnham, F. Al-Beidh, S. Santhakumaran, S. J. Brett, C. J. Hinds, D. Ashby, J. C. Knight, A. C. Gordon, Transcriptomic signatures in sepsis and a differential response to steroids. From the VANISH randomized trial. *American journal of respiratory and critical care medicine* **199**, 980-986 (2019).
64. C. S. Calfee, K. L. Delucchi, P. Sinha, M. A. Matthay, J. Hackett, M. Shankar-Hari, C. McDowell, J. G. Laffey, C. M. O'Kane, D. F. McAuley, Acute respiratory distress syndrome subphenotypes and differential response to simvastatin: secondary analysis of a randomised controlled trial. *The Lancet Respiratory Medicine* **6**, 691-698 (2018).
65. D. S. Gruen, J. B. Brown, F. X. Guyette, Y. Vodovotz, P. I. Johansson, J. Stensballe, D. A. Barclay, J. Yin, B. J. Daley, R. S. Miller, B. G. Harbrecht, J. A. Claridge, H. A. Phelan, M. D. Neal, B. S. Zuckerbraun, T. R. Billiar, J. L. Sperry, Prehospital plasma is associated with distinct biomarker expression following injury. *JCI Insight* **5**, (2020).
66. M. Nguyen, R. Pirracchio, L. Z. Kornblith, R. Callcut, E. E. Fox, C. E. Wade, M. Schreiber, J. B. Holcomb, J. Coyle, M. Cohen, A. Hubbard, Dynamic impact of transfusion ratios on outcomes in severely injured patients: Targeted machine learning analysis of the Pragmatic, Randomized Optimal Platelet and Plasma Ratios randomized clinical trial. *J Trauma Acute Care Surg* **89**, 505-513 (2020).
67. S. A. Christie, A. S. Conroy, R. A. Callcut, A. E. Hubbard, M. J. Cohen, Dynamic multi-outcome prediction after injury: Applying adaptive machine learning for precision medicine in trauma. *PloS one* **14**, e0213836 (2019).
68. R. Pirracchio, M. J. Cohen, I. Malenica, J. Cohen, A. Chambaz, M. Cannesson, C. Lee, M. Resche-Rigon, A. Hubbard, Big data and targeted machine learning in action to assist medical decision in the ICU. *Anaesth Crit Care Pain Med* **38**, 377-384 (2019).
69. S. A. Christie, A. E. Hubbard, R. A. Callcut, M. Hameed, F. N. Dissak-Delon, D. Mekolo, A. Saidou, A. C. Mefire, P. Nsongoo, R. A. Dicker, M. J. Cohen, C. Juillard, Machine learning without borders? An adaptable tool to optimize mortality prediction in diverse clinical settings. *J Trauma Acute Care Surg* **85**, 921-927 (2018).
70. A. D. Grossman, M. J. Cohen, G. T. Manley, A. J. Butte, Infection in the intensive care unit alters physiological networks. *BMC Bioinformatics* **10 Suppl 9**, S4 (2009).
71. M. J. Cohen, A. D. Grossman, D. Morabito, M. M. Knudson, A. J. Butte, G. T. Manley, Identification of complex metabolic states in critically injured patients using bioinformatic cluster analysis. *Crit Care* **14**, R10 (2010).

Funding: This study was supported by funds from the National Institutes of General Medical Sciences (NIGMS), award no. RM1GM131968 to CCS, KCH, EEM, MC, ADA and the award no. P50GM049222 (EEM, CCS, KCH). Additional support was provided by the Department of Defense DoD, award no. W81XWH-12-2-0028 to EEM.

Author contributions:

Conceptualization: All authors

Methodology: MJC, CBE, ISL, ADA, KCH

Investigation: All authors

Visualization: CBE, ISL

Funding acquisition: EEM, CCS, KCH, MC, ADA

Supervision: EEM, CCS, ADA, KCH

Writing – original draft: MJC, CBE, ADA, KCH

Writing – review & editing: All authors

Competing interests: ADA and KCH are founders of Omix Technologies Inc. ADA is a scientific advisory board member for Hemanext Inc and Macopharma Inc. All the other authors have no conflicts to disclose.

Data and materials availability: All data are available in **Supplementary Table 1**. Raw Proteomics, Metabolomics data will be made publicly available via Metabolomics

Workbench and PRIDE upon acceptance and final publication. Code will be uploaded to Zenodo upon final publication.

FIGURES

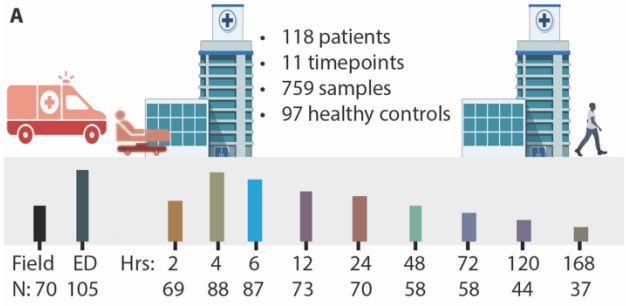

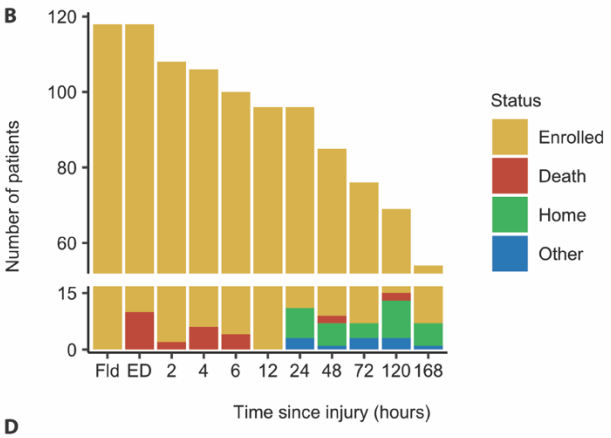

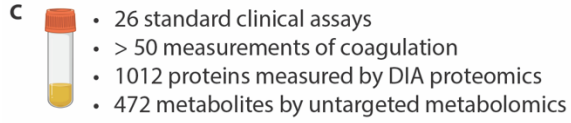

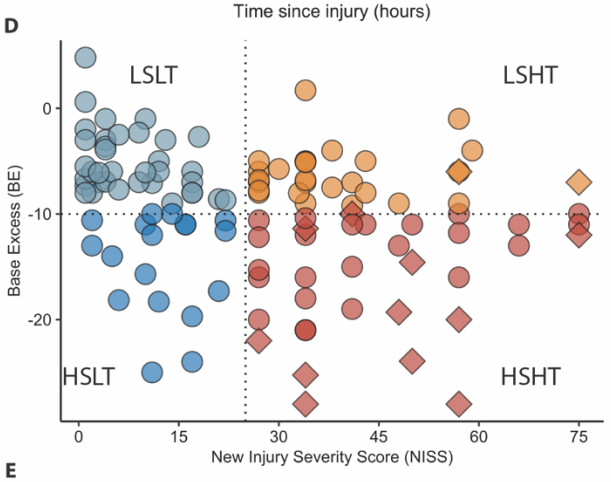

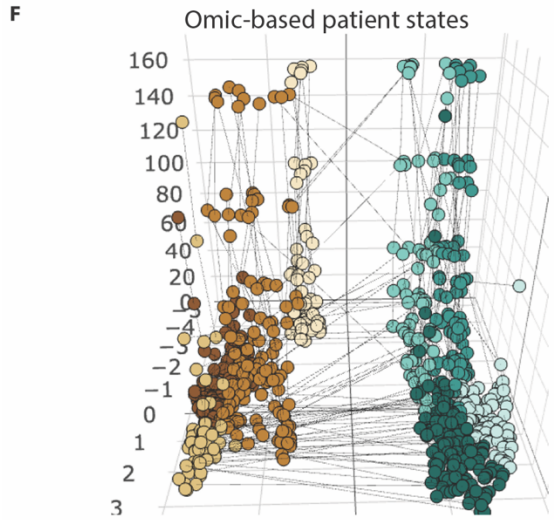

E

Characteristic	LSHT	HSHT	HSLT	LSLT
n	28	35	18	36
Age years (IQR)	33 (24.8)	29 (20.5)	41.5 (17.8)	32.5 (18)
BMI (IQR)	27.1 (8.9)	26.9 (5.0)	27.5 (4.9)	24.4 (6.0)
M% (M/F)*	71% (20/8)	83% (29/6)	94% (17/1)	83% (30/6)
Comorbid% (y/n)*	14% (4/24)	11% (4/31)	28% (5/13)	11% (4/32)
Blunt %*	71%	57%	22%	42%
Penetrating %*	25%	43%	78%	56%
NISS (IQR)*	34 (12)	41 (23)	11.5 (6.75)	5.5 (10.3)
BE (IQR)*	-6.8 (2.8)	-14.6 (8.7)	-12.5 (6.9)	-6 (4.1)
TBI% (y/n)'8	14% (4/23)	29% (10/25)	0% (0/18)	0% (0/36)
HR BPM (IQR)*	95 (50)	122 (32.5)	123 (22)	104 (35)
SBP mmHg (IQR)	94 (58.5)	90 (35)	92 (22.5)	108 (39.5)
Temp C (IQR)	36.5 (0.31)	36.25 (0.63)	36.5 (0.48)	36.7 (0.45)
GCS (IQR)*	15 (5.5)	3 (9.5)	15 (2)	15 (1)
HGB g/dL (IQR)	13.4 (2.4)	11.9 (4.1)	12.1 (3.9)	13.6 (2.3)
Platelets x10^3/μL*	229 (89)	215 (116)	189 (128)	283 (121
INR (IQR)*	1.16 (0.23)	1.35 (0.38)	1.28 (0.29)	1.12 (0.17)
MTX% (y/n)*	4% (1/26)	29% (10/25)	0% (0/18)	0% (0/36)
Hospital days*	14 (13.4)	11 (29.5)	8.5 (8.75)	3 (6)
ICU-free days (IQR)*	21.5 (14)	9 (20.5)	24.5 (7.25)	28 (3)
Vent-free days (IQR)*	25 (14.5)	13 (24)	27 (3.5)	28 (1)
Death (%)*	7% (2/26)	31% (11/24)	0% (0/18)	0% (0/36)

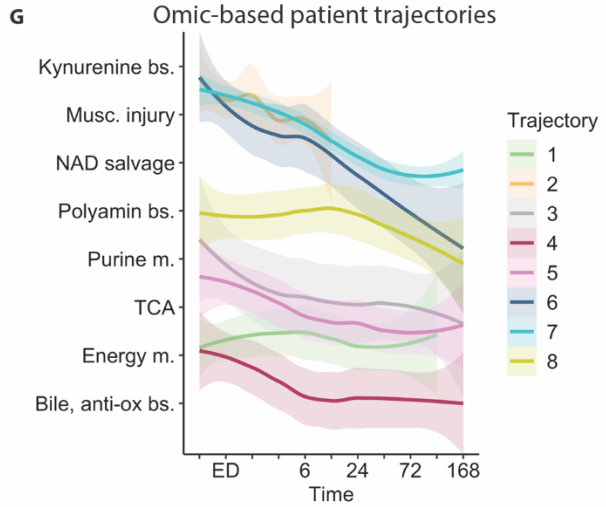

Figure 1 caption: Overview of data collection, study design, and patient characteristics. (**A**) Patients who met the COMBAT criteria for shock and trauma were enrolled at the Field timepoint. Blood was collected in the Field, and at 10 subsequent timepoints. (**B**) The number of patients currently enrolled, deceased, or discharged varied by timepoint. (**C**) Blood collected at each timepoint was processed for LC-MS/MS proteomics and metabolomics, and also for routine clinical blood chemistry assays. (**D**) Patients were categorized into Shock/Trauma (S/T) groups Low-Shock-Low-Trauma (LSLT); Low-Shock-High-Trauma (LSHT); High-Shock-Low-Trauma (HSLT); or High-Shock-High-Trauma (HSHT) based on NISS and BE at ED arrival (NISS >= 25 is HT; BE <= -10 is HS); diamond is deceased. (**E**) Clinical characteristics and clinical blood chemistry measurements are outlined with median values +/- IQR (*$p<0.05$, ANOVA, TukeyHSD post-hoc) , or percent (% *$p<0.05$, χ^2). (**F-G**) S/T groups were then compared to outcomes based on unsupervised clustering of omic data followed by prediction learning to identify omic-based patient trends and outcome trajectories.

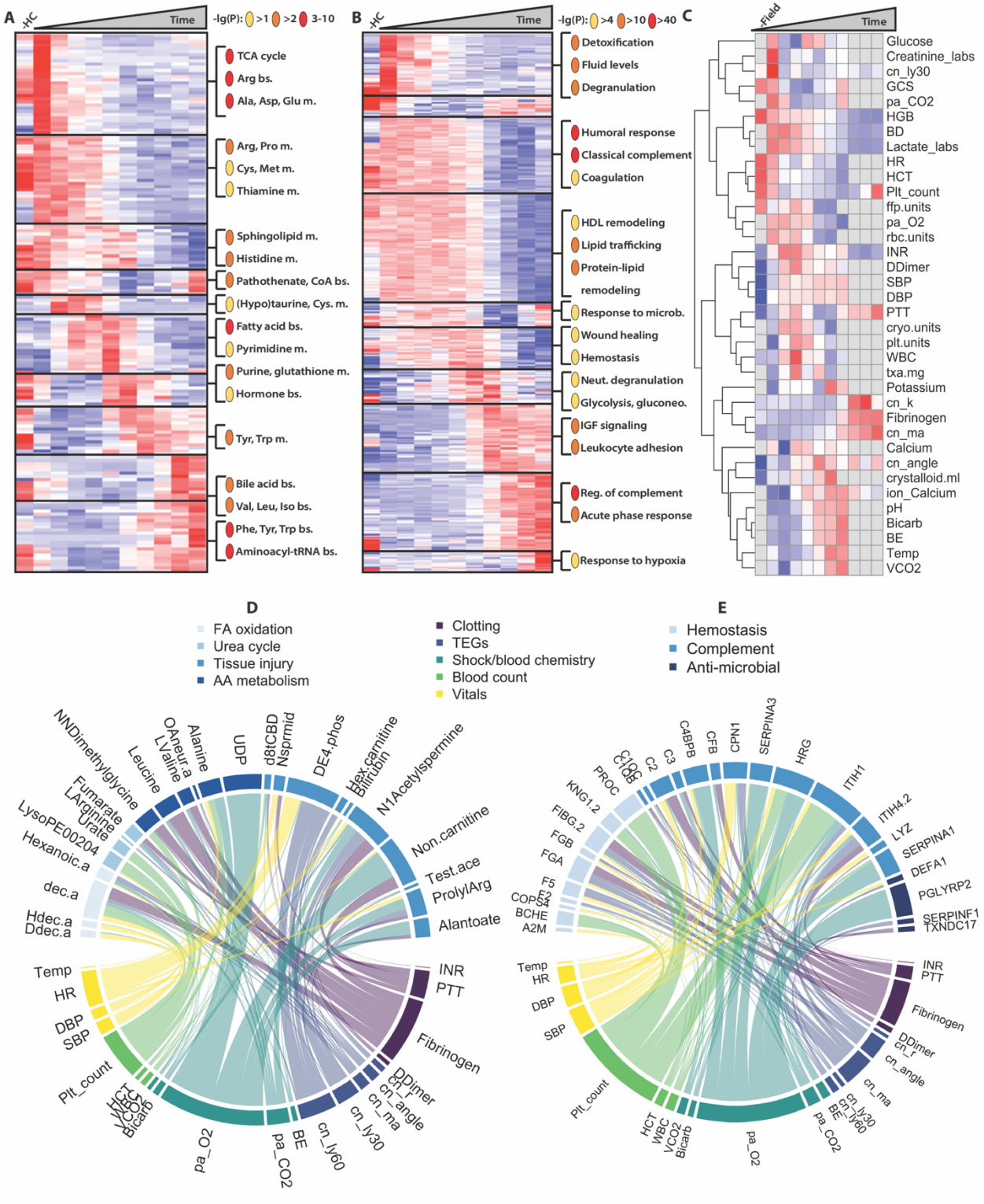

Figure 2 caption: Metabolomic, proteomic, and clinical trends of the "average" trauma patient. (**A**) Heatmap of median values of metabolites sharing similar temporal, kinetic patterns from C-means clustering (left side); and enrichment terms of each cluster (right side, enrichment scores from MetaboAnalyst). (**B**) Heatmap of median values of proteins sharing similar temporal,

kinetic patterns from C-means clustering (left side); and GO enrichment terms of each cluster (right side, enrichment scores from Metascape). (**C**) Clinical chemistry labs showing the relative, median value at each timepoint. (**D-E**) Strength of association (partial slope from mixed modeling) between clinical measurements and associated metabolites D) or proteins E), with line thickness showing relative partial slope. dec.a = Decanoic acid. Ddec.a = Dodecanoic acid. Hdec.a = Hexadecenoic acid. Hexanoic.a = Hexanoic acid. OAneur.a = OAcetylneuraminic.acid. d8tCBD = delta-8-tetrahydrocannabinol. Nsprmid = N1-Acetylspermidine. Hex.carnitine = Hexenoylcarnitine. Non.carnitine = Nonanoylcarnitine. DE4.phos = DErythrose.4phosphate. Test.ace = Testosterone.acetate. ProlylArg = Prolyl-Arginine. TEG = Thromboelastography.

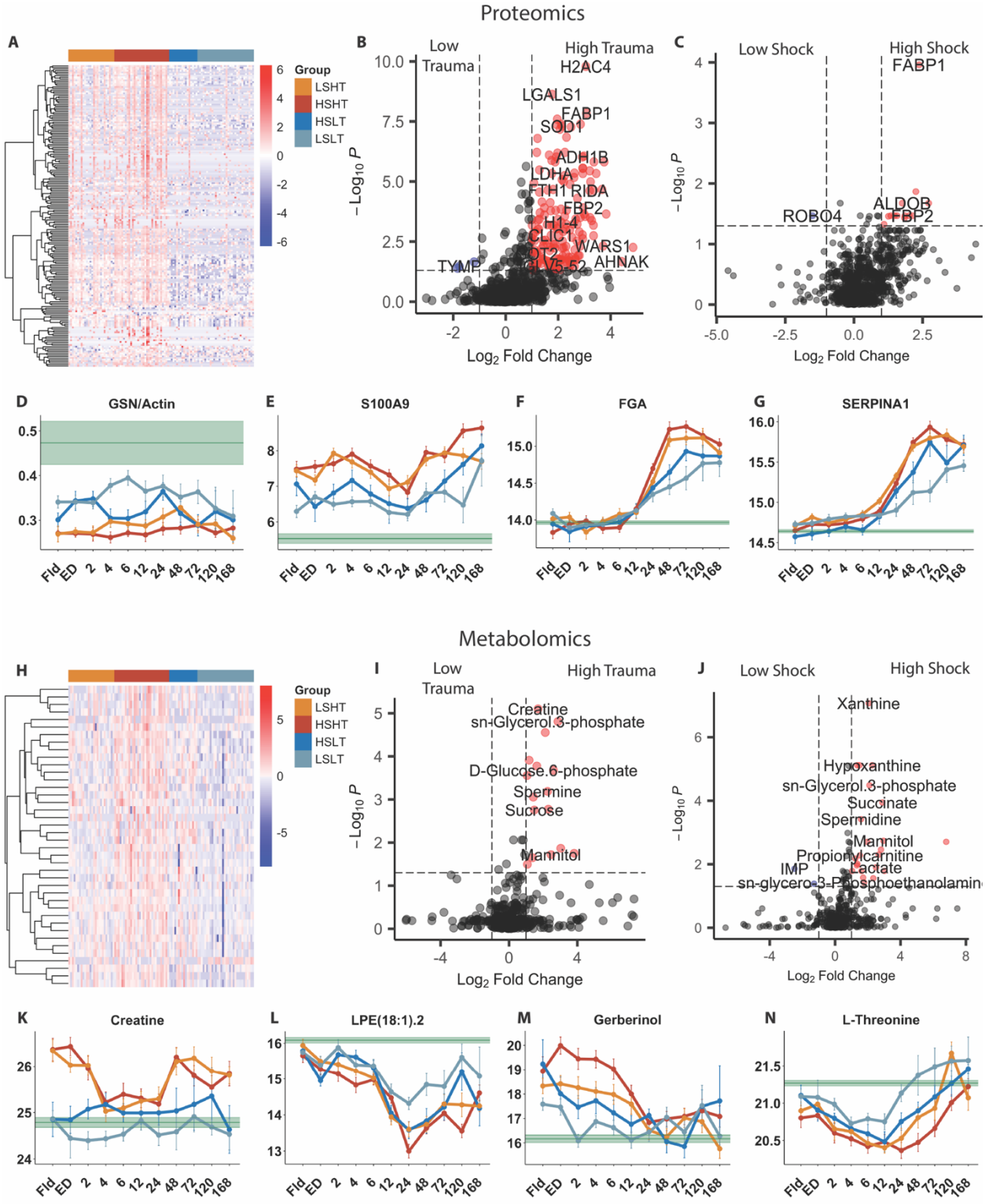

Figure 3: Golden hour trauma patient plasma omics. (**A**) Proteomic heatmap of significant analytes at ED by S/T group (FDR-corrected p<0.05 following ANOVA). (**B**) Proteomic volcano plot between HT (right. N=63) vs. LT (left N = 54) colored by significance (FDR-corrected p<0.05 following t-test) and relative fold change (red for HT/LT > 2x; blue for LT/HT > 2x). (**C**)

Proteomic volcano plot between HS (right. N=53) vs. LS (left. N=64) colored by significance (FDR-corrected $p<0.05$ following t-test) and relative fold change (red for HS/LS > 2x; blue for LS/HS > 2x). (**D-G**) Line plots of median +/-SEM of tissue injury (GSN/Actin), detox (S100A9), clotting (FGA), and protease inhibitor (SERPINA1) proteins over time (*$p<0.05$ Sidak correction on estimated marginal means of mixed model). Green line = HC values. (**H-J**) Similar analysis for metabolomics showing S/T heatmap (H), and HT/LT (I) and HS/LS (J) volcano plots at ED. (**K-N**) Line plots of metabolites involved in tissue injury (creatine), lipid synthesis (LPE(18:1)), hypoxia (spermidine), protein synthesis (L-Threonine).

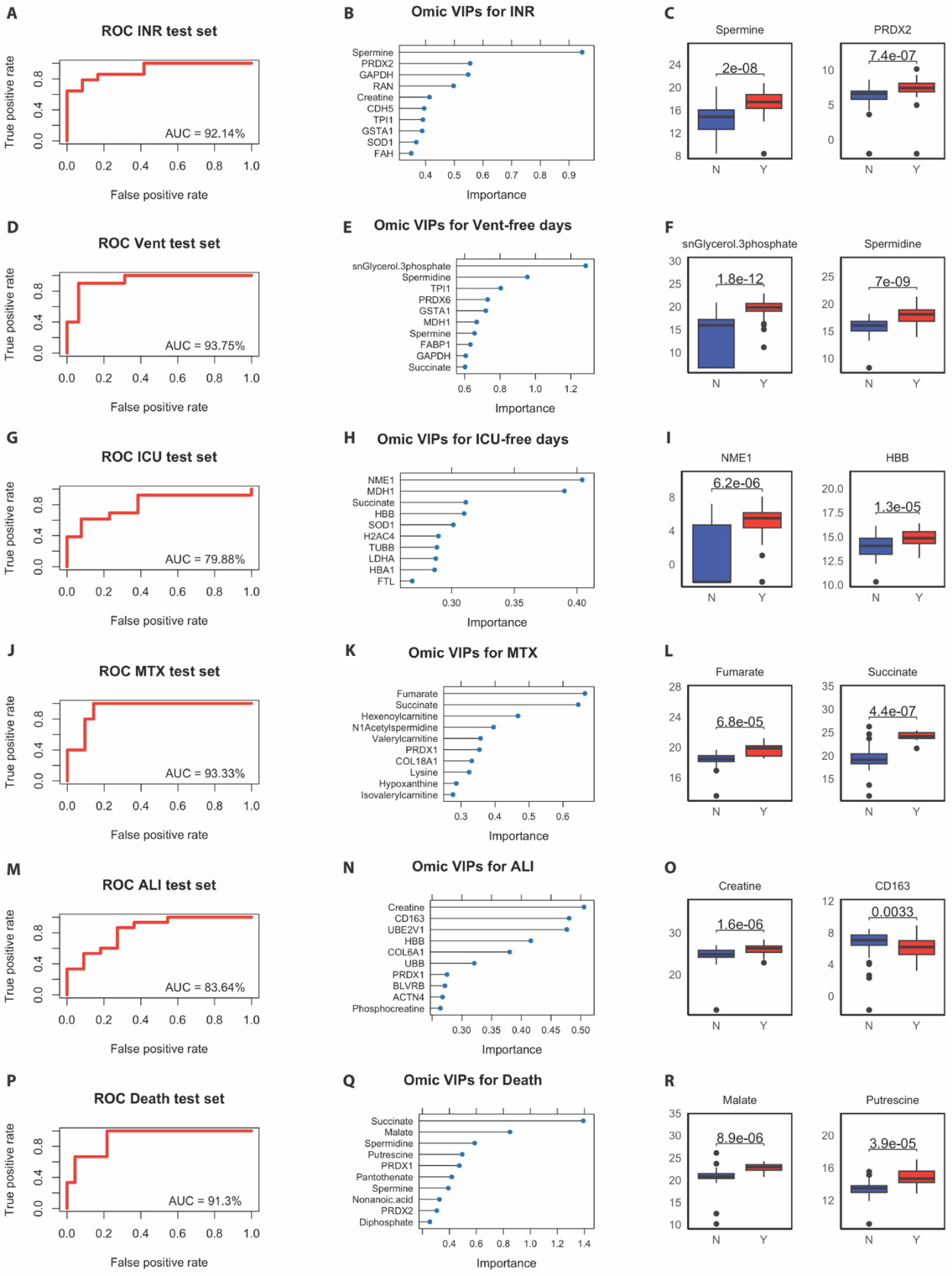

Figure 4: Ensemble learning to predict patient outcomes. Ensemble models were trained and tested on separate sets of ED data to predict patient outcomes, and identify important analytes (VIP analysis from RandomForest) contributing to outcomes. ROC analysis of Ensemble model performance with AUC (1st column), VIP analysis (2nd column), and boxplots of top VIP analytes (3rd column, t-test) identified to predict (**A-C**) coagulopathy by INR, (**D-F**) Ventilator-free days, (**G-I**) ICU-free days, (**J-K**) the need for massive transfusion (MTX), (**M-O**) acute lung injury (ALI), and (**P-R**) death.

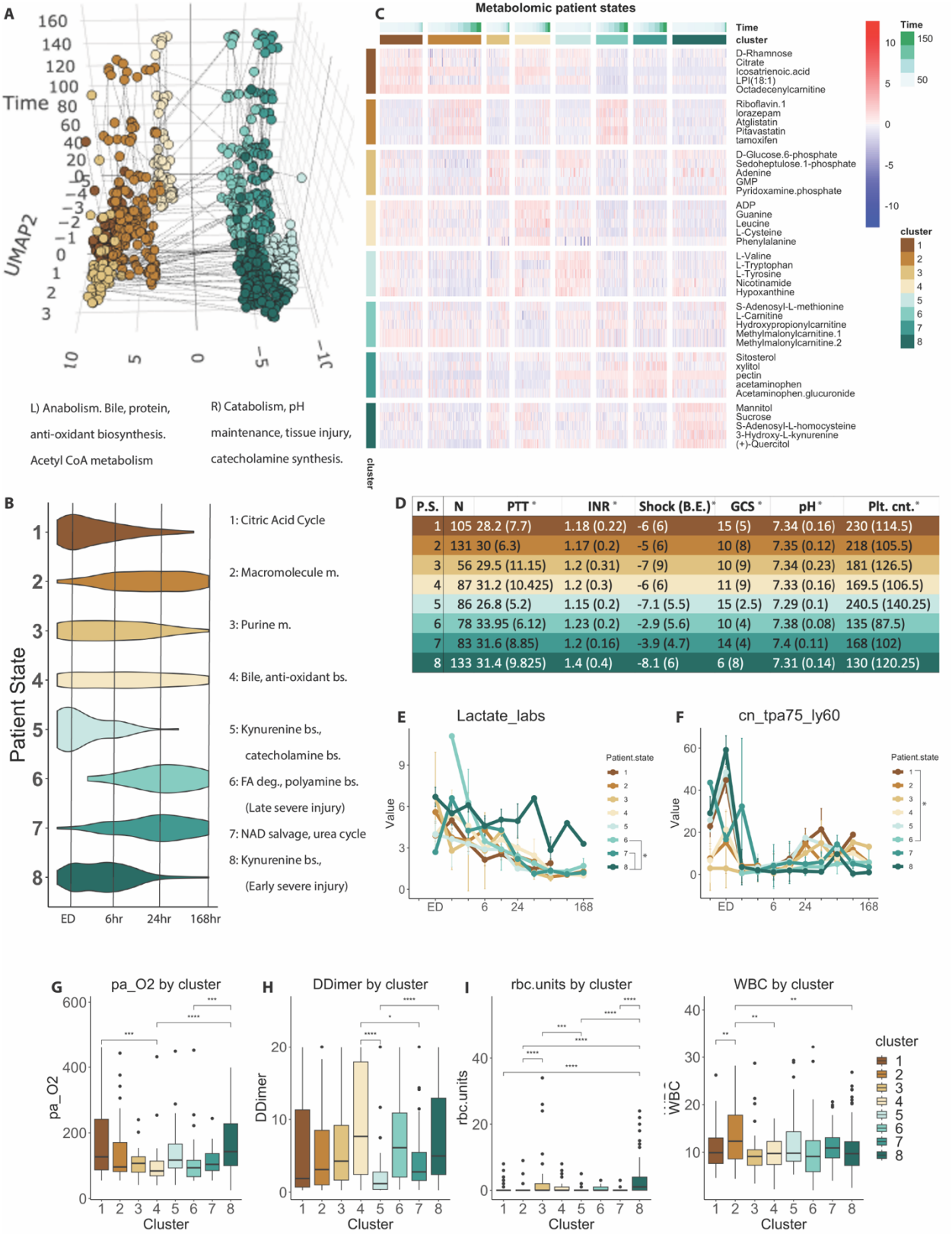

P.S.	N	PTT *	INR *	Shock (B.E.)*	GCS *	pH *	Plt. cnt.*
1	105	28.2 (7.7)	1.18 (0.22)	-6 (6)	15 (5)	7.34 (0.16)	230 (114.5)
2	131	30 (6.3)	1.17 (0.2)	-5 (6)	10 (8)	7.35 (0.12)	218 (105.5)
3	56	29.5 (11.15)	1.2 (0.31)	-7 (9)	10 (9)	7.34 (0.23)	181 (126.5)
4	87	31.2 (10.425)	1.2 (0.3)	-6 (6)	11 (9)	7.33 (0.16)	169.5 (106.5)
5	86	26.8 (5.2)	1.15 (0.2)	-7.1 (5.5)	15 (2.5)	7.29 (0.1)	240.5 (140.25)
6	78	33.95 (6.12)	1.23 (0.2)	-2.9 (5.6)	10 (4)	7.38 (0.08)	135 (87.5)
7	83	31.6 (8.85)	1.2 (0.16)	-3.9 (4.7)	14 (4)	7.4 (0.11)	168 (102)
8	133	31.4 (9.825)	1.4 (0.4)	-8.1 (6)	6 (8)	7.31 (0.14)	130 (120.25)

Figure 5: Metabolomic patient states. (**A**) 3D UMAP of clustered metabolomic data stratified by timepoint; two meta groups generally defined by biosynthesis of macromolecules (L) versus elevated catabolism (R). (**B**) Patient states vary temporally with early injury (states 1, 5, 8), mid-injury (2, 3, 4), and late-injury (6, 7) enriched clusters. (**C**) Each state had a significantly elevated metabolite signature that enriched for different cellular metabolic processes. Top 5 shown, full list in Figure S14 (**D**) Clinical measurements for each metabolic state is outlined as median +/-IQR (*$p<0.05$ via ANOVA, TukeyHSD post-hoc). (**E-J**) Line graphs (*$p<0.05$ Sidak correction on estimated marginal means of mixed models) showing temporal trends and (**G-J**) box plots showing static trends (*$p<0.05$ by ANOVA, TukeyHSD post-hoc) of clinically relevant measurements. Full list of clinical results in SF15.

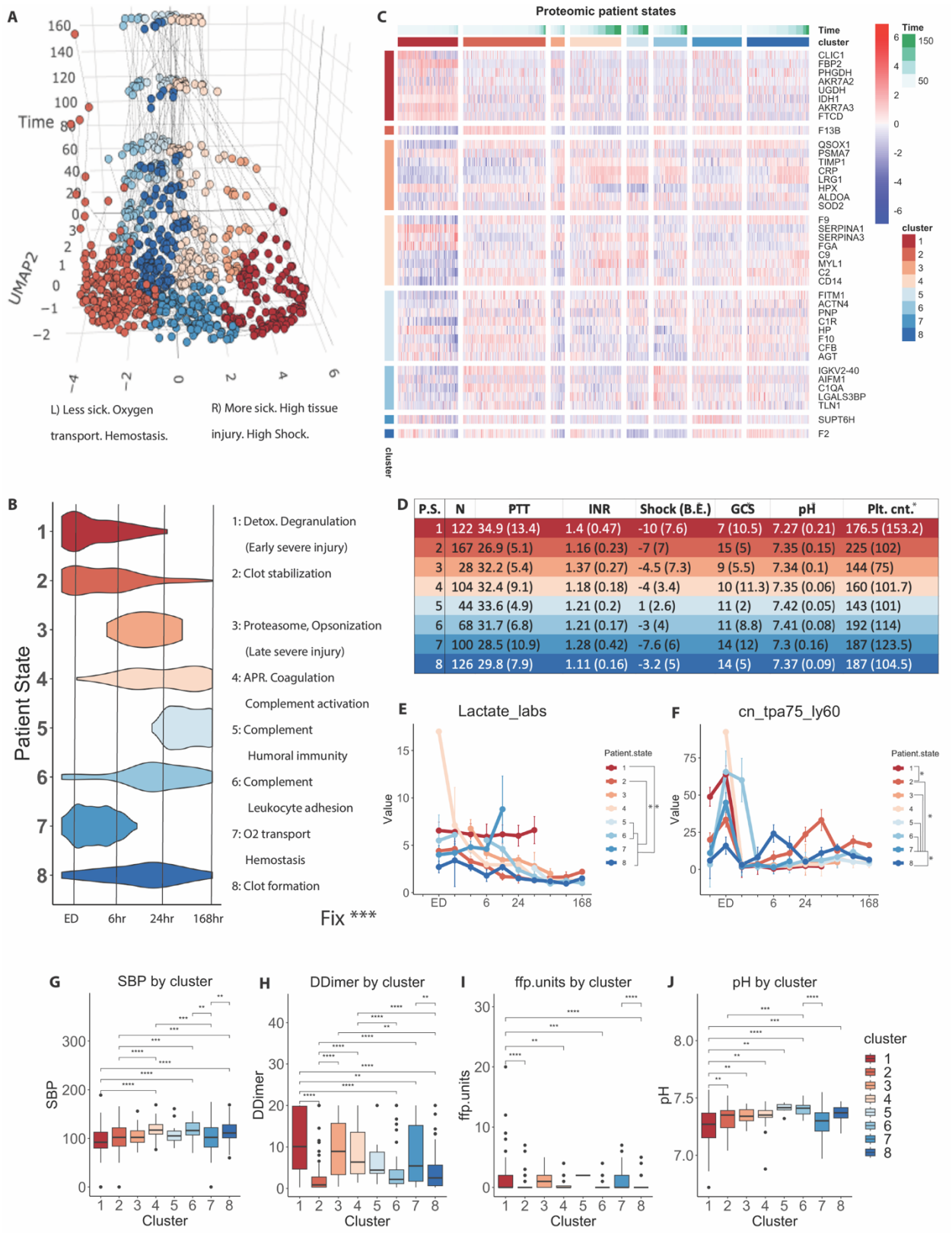

P.S.	N	PTT	INR	Shock (B.E.)	GCS	pH	Plt. cnt.*
1	122	34.9 (13.4)	1.4 (0.47)	-10 (7.6)	7 (10.5)	7.27 (0.21)	176.5 (153.2)
2	167	26.9 (5.1)	1.16 (0.23)	-7 (7)	15 (5)	7.35 (0.15)	225 (102)
3	28	32.2 (5.4)	1.37 (0.27)	-4.5 (7.3)	9 (5.5)	7.34 (0.1)	144 (75)
4	104	32.4 (9.1)	1.18 (0.18)	-4 (3.4)	10 (11.3)	7.35 (0.06)	160 (101.7)
5	44	33.6 (4.9)	1.21 (0.2)	1 (2.6)	11 (2)	7.42 (0.05)	143 (101)
6	68	31.7 (6.8)	1.21 (0.17)	-3 (4)	11 (8.8)	7.41 (0.08)	192 (114)
7	100	28.5 (10.9)	1.28 (0.42)	-7.6 (6)	14 (12)	7.3 (0.16)	187 (123.5)
8	126	29.8 (7.9)	1.11 (0.16)	-3.2 (5)	14 (5)	7.37 (0.09)	187 (104.5)

Figure 6: Proteomic patient states. (**A**) 3D UMAP of clustered proteomic data stratified by timepoint with sicker (R), and less sick (L) sides. (**B**) Patient states varied temporally with early

injury (states 1, 2, 7), mid-injury (3, 8), and late-injury (4, 5, 6) enriched clusters. (**C**) Each state had a significantly elevated proteomic signature that enriched for different GO processes. (**D**) Clinical measurements for each proteomic state is outlined as median +/-IQR (*$p<0.05$ via ANOVA, TukeyHSD post-hoc). (**E-J**) Line graphs (*$p<0.05$ Sidak correction on estimated marginal means of mixed models) showing temporal trends and (**G-J**) box plots showing static trends (*$p<0.05$ by ANOVA, TukeyHSD post-hoc) of clinically relevant measurements. Full list in SF16.

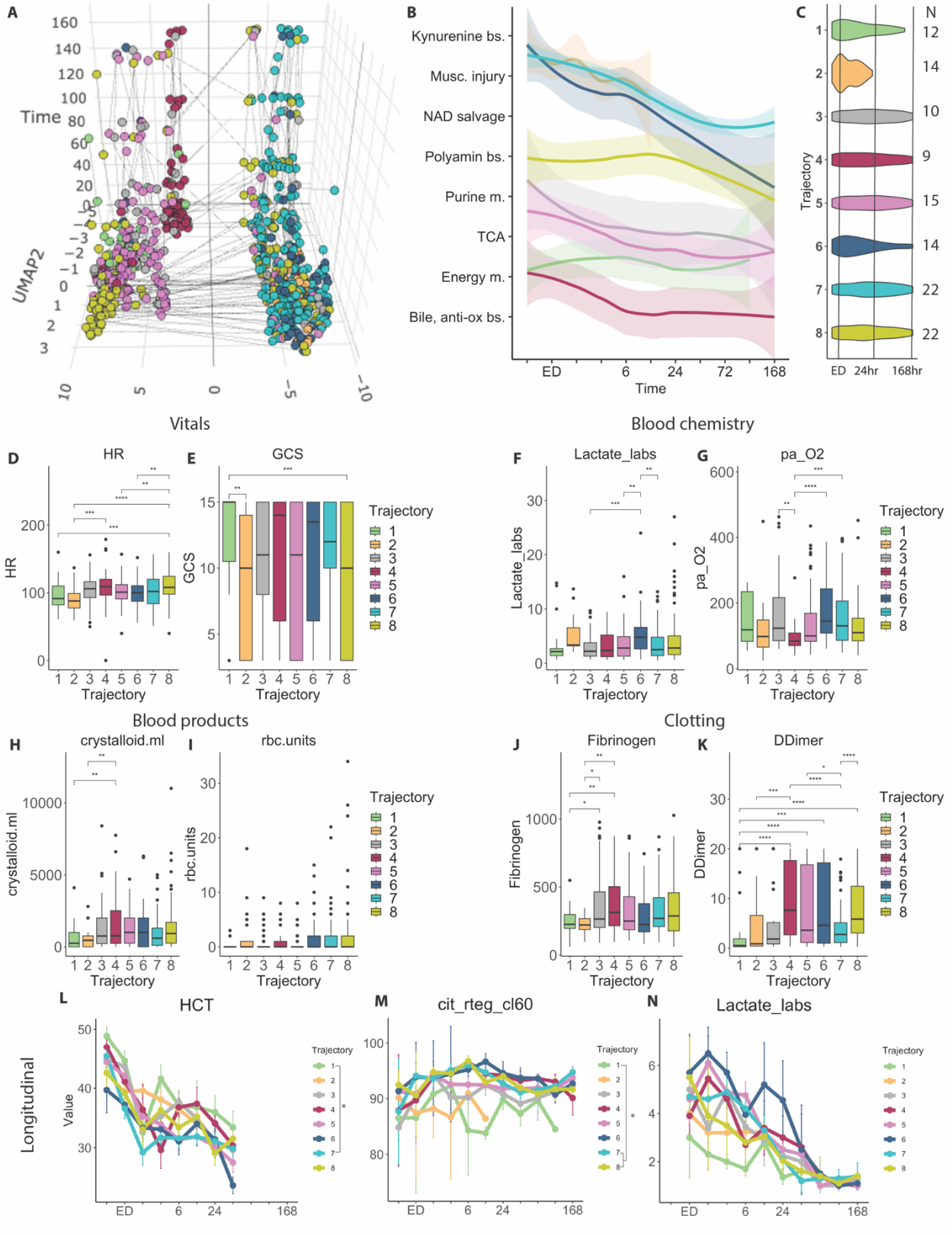

Figure 7: Metabolomic patient trajectories. (**A**) UMAP colored by metabolomic patient trajectories. (**B**) Line plot of each trajectory through metabolomic patient state space +/- 95% CI; x-axis is time, y-axis is patient state. (**C**) Temporal nature of trajectories, with most patients in trajectories 2 and 6 leaving relatively early. (**D-K**) Box plots (*$p<0.05$ ANOVA, TukeyHSD post-hoc) and line graphs (*$p<0.05$ Sidak correction on estimated marginal means of mixed models) showing temporal trends of clinically relevant measurements for each trajectory.

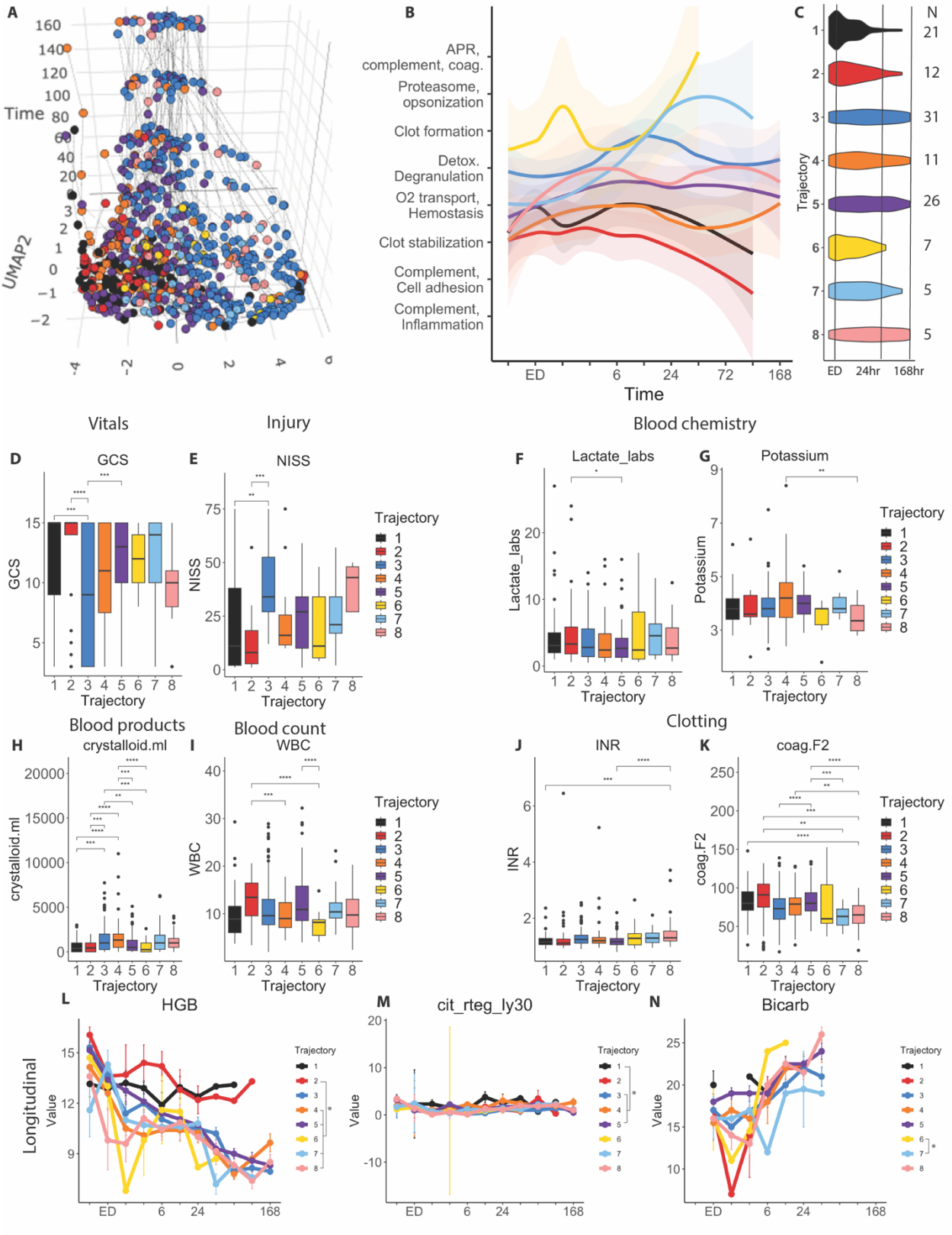

Figure 8: Proteomic patient trajectories. (**A**) UMAP colored by proteomic patient trajectories. (**B**) Line plot of each trajectory through proteomic patient state space +/- 95% CI; x-axis is time, y-axis is patient state. (**C**) Temporal nature of trajectories. (**D-K**) Box plots (*p<0.05 ANOVA, TukeyHSD post-hoc) and line graphs (*p<0.05 Sidak correction on estimated marginal means of mixed models) showing temporal trends of clinically relevant measurements for each trajectory.